

Dust and Diffuse Interstellar Bands in the $z_a = 0.524$ Absorption System toward AO 0235+164^{1,2}

V. T. Junkkarinen, Ross D. Cohen, E. A. Beaver, E. M. Burbidge, R. W. Lyons

Center for Astrophysics and Space Sciences, University of California, San Diego, La Jolla, CA 92093-0424

vesa@ucsd.edu, rdcohen@ucsd.edu

G. Madejski

Stanford Linear Accelerator Center, 2575 Sand Hill Road, Menlo Park, CA 94025

ABSTRACT

We present new HST STIS NUV–MAMA and STIS CCD observations of the BL Lac object AO 0235+164 and the intervening damped Ly α (DLA) line at $z_a = 0.524$. The line profile gives $N(HI) = 5 \pm 1 \times 10^{21} \text{ cm}^{-2}$ and, combined with the H I 21 cm absorption data leads to a spin temperature of $T_s = 220 \text{ K} \pm 60 \text{ K}$. Those spectra also show a strong, broad feature at the expected position of the 2175 Å graphitic dust feature at $z_a = 0.524$. Assuming a Galactic type dust extinction curve at $z_a = 0.524$ gives a dust-to-gas ratio of 0.19 Galactic, but the fit, assuming the underlying, un-reddened spectrum is a single power-law, is poor in the far-UV. A dust-to-gas ratio of 0.19 Galactic is similar to the LMC, but the AO 0235+164 spectrum does not fit the LMC extinction curve, or the SMC extinction curve (which has practically no 2175 Å feature). A possible interpretation includes dust similar to Galactic, but with less of the small particles that produce the far-UV extinction. The metallicity of the $z_a = 0.524$ absorber, estimated from the observed $N(HI)$ and excess X-ray absorption (beyond Galactic) derived from contemporaneous and archival ASCA and ROSAT

¹Based on observations with the NASA/ESA Hubble Space Telescope, obtained at the Space Telescope Science Institute, which is operated by the Association of Universities for Research in Astronomy, Inc. under NASA contract No. NAS5–26555.

²Some of the data presented herein were obtained at the W. M. Keck Observatory which is operated as a scientific partnership among the California Institute of Technology, the University of California and the National Aeronautics and Space Administration. The Observatory was made possible by the generous financial support of the W. M. Keck Foundation.

X-ray data, is $Z = 0.72 \pm 0.28 Z_{\odot}$, implying in turn the dust-to-metals ratio of 0.27 Galactic. If the dust mass density is the same in the $z_a = 0.524$ DLA system as in our Galaxy, only 14% ($\pm 6\%$) of the metals (by mass) are in dust compared with 51%, 36%, and 46% for the Galaxy, LMC, and SMC respectively. Such a dusty $z_a = 0.524$ AO 0235+164 absorption system is a good example of the kind of DLA system that will be missed due to selection effects, which in turn can bias the measurement of the co-moving density of interstellar gas (in units of the closure density), Ω_g , as a function of z .

Subject headings: galaxies: ISM – galaxies: abundances – quasars: absorption lines – quasars: individual (AO 0235+164)

1. Introduction

Dust in damped Ly α (DLA) systems has important implications for studies of the chemical evolution of the universe (Pei and Fall 1995). Dust absorption is correlated with metallicity so the more metal rich systems will be underrepresented in DLA surveys using magnitude limited samples of background targets. Evidence for dust in DLA systems comes from the statistics of the spectral slopes of the background quasars. Quasars with DLA systems have, on average, redder spectra (Fall and Pei 1989; Fall, Pei, and McMahon 1989). The background control quasars have a range of spectral slopes, so the confirmation of reddening in any individual DLA system is usually not possible by this method.

Evidence for dust in DLA systems also comes from studies of the column density ratios of certain ions, in particular Cr II/Zn II (Pettini et al. 1994, 1997a). Cr is more readily depleted by grain formation than Zn which normally undergoes very little dust depletion. Pettini et al. (1997a, 1999) find low metallicities based on Zn, with $[\langle \text{Zn}/\text{H} \rangle]^1 = -1.03$ for $z < 1.5$, a large scatter, and little or no evolution of metallicity with redshift. The dust content in these low metallicity systems is low mainly because the systems are low metallicity but also because the available metals are not efficiently converted to dust. Based on Cr II/Zn II and other line ratios, the dust-to-metals ratio is estimated to be ~ 0.5 times that of the local Galactic ISM (Pettini et al. 1997a). The combination of low metallicity and the 0.5 fractional dust-to-metals ratio relative to Galactic leads to the result that dust should mainly show up in DLA systems in the selective depletion of certain elements, like Cr, while the typical extinction due to dust is small, $A_{1500} \sim 0.1$ (Pettini et al. 1997a). However, there

¹Where $[\text{A}/\text{H}]$ is the base 10 logarithm of the abundance ratio of A/H divided by the solar A/H ratio.

is still some uncertainty in the interpretation of the observed element abundances in DLA systems because the overall pattern may not match the combined effect of early α process (SNe II) enhancement combined with dust depletion (e.g. Lu et al. 1996; Prochaska and Wolfe 1999). There may be a problem with the use of Zn as a metallicity indicator because super-solar values of $[\text{Zn}/\text{Fe}]$ might result from early Zn production by SNe II nucleosynthesis (Prochaska and Wolfe 2000). If Zn is not a good metallicity indicator, then $[\text{Cr}/\text{Zn}]$ is an unreliable indicator of dust when Cr is apparently depleted by only a small amount relative to Zn.

A more direct detection of dust in individual DLA systems is possible by the observation of the 2175 Å dust feature thought to be produced by graphitic dust grains (Draine 1993; Will and Aannestad 1999). Somewhat less direct evidence for dust is the presence of diffuse interstellar bands (DIBs) which are known to correlate with $E(B - V)$ and other dust indicators in our Galaxy (e.g. Herbig 1995). DIBs have been observed in only a few extragalactic objects: the LMC (Vladilo et al. 1987) and NGC 5128 (Cen A) (D’Odorico et al. 1989) and toward some dusty starburst galaxies (Heckman and Lehnert 2000).

A search for the 2175 Å feature in a sample of quasars with DLA systems by Pei, Fall, and Bechtold (1991) yielded no detections. Pei et al. suggest that Galactic type dust is ruled out in these systems and that the dust absorption may have an extinction curve similar to that associated with either the Small Magellanic Cloud or the Large Magellanic Cloud. The SMC extinction has essentially no 2175 Å feature while the LMC extinction has a weaker 2175 Å extinction feature relative to Galactic extinction (e.g. Pei 1992).

A broad 2175 Å feature has been detected by Malhotra (1997) in a composite spectrum created by aligning 96 quasar Mg II absorption systems. The nature of the composite spectrum and the relatively shallow feature found by Malhotra (1997) make any dust-to-gas ratio and extinction curve determination very uncertain. A Galactic type 2175 Å feature has recently been discovered in a quasar absorption system at $z_a = 0.83$ by Motta et al. (2002). This system was found in the analysis of the spectra of the gravitationally lensed quasar SBS 0909+532. The 2175 Å feature is apparent in the ratio of the spectra from the two lines-of-sight. Such lines-of-sight are very valuable for determining extinction curves because the extinction can be determined independently of the underlying spectral shape. Because the absorption is probably due to the lensing galaxy (Motta et al. 2002), the selection properties of these systems differ from the absorption survey selected high column density and DLA absorbers.

AO 0235+164 is a well studied BL Lac object that shows high amplitude optical variability (Rieke et al. 1976), rapid X-ray variability (Madejski et al. 1996), strong GeV γ -ray emission (Hunter et al. 1993), and possible VLBA radio components that move with

apparent superluminal expansion velocities (Marscher and Machenko 1999). AO 0235+164 has characteristics consistent with a fairly extreme example of a blazar, which are thought to be AGN with a jet aligned closely to our line-of-sight (e.g. Urry 1999). More specifically, given that AO 0235+164 was selected by radio emission and has a relatively low ratio of X-ray flux to 100 Mev γ -ray flux (Madejski et al. 1996), AO 0235+164 is probably best described as a “red” or, equivalently, a low-frequency peaked BL Lac object (e.g. Urry 1999). In its low state AO 0235+164 shows weak emission lines at $z_e = 0.94$ (Cohen et al. 1987). Sometimes, when the continuum emission is very weak, the emission line equivalent widths are large enough that AO 0235+164 could be classified as an optically violent variable (OVV) quasar (Nilsson et al. 1996).

During a particularly bright flare in 1975, when AO 0235+164 reached $V = 14.3$ (Rieke et al. 1976), optical observations showed absorption systems at $z_a = 0.524$ and $z_a = 0.852$ (Rieke et al. 1976; Burbidge et al. 1976). The $z_a = 0.524$ absorption system has a high H I column density; strong multicomponent H I 21 cm absorption was detected against the background radio source (Roberts et al. 1976). The 21 cm H I absorption is time variable (Wolfe, Davis, and Briggs 1982). The radio observations combined with a measurement of the H I column density from the DLA line at $\lambda_{obs} = (1 + z_a) 1216 \text{ \AA} = 1853 \text{ \AA}$ can be used to estimate the spin temperature T_s of the gas producing the absorption. The measurement of the DLA line has been the goal of several investigations. The DLA line at $z_a = 0.524$ was observed with IUE yielding $N(HI) = 3 \times 10^{21} \text{ cm}^{-2}$ with factor of 2 errors from a very noisy spectrum (Snijders et al. 1982). The HST FOS GTO group at UCSD attempted to obtain a higher S/N UV spectrum of AO 0235+164 in July 1995. At the time of the attempted observations, AO 0235+164 had varied to a historically faint apparent brightness around $V = 20.5$ (Burbidge et al. 1996). The field of AO 0235+164 has a Seyfert type emission line galaxy, called object A, with $z_e = 0.524$ about 2 arcsec south of the BL Lac object (Smith, Burbidge, and Junkkarinen 1977). The FOS target acquisition aperture included both AO 0235+164 and object A, and object A was brighter. The end result of the July, 1995 FOS observation was a spectrum of object A which shows not only strong AGN type emission lines but also broad associated absorption (Burbidge et al. 1996).

In this paper we report results from a GTO HST STIS program (GO-7294, PI R.D. Cohen) and Asca observation to obtain UV, X-ray and optical spectra of AO 0235+164. These spectra, obtained in February, 1998 when AO 0235+164 was relatively bright, $V \sim 16.4$, not only provide a measurement of $N(HI)$ from the DLA line at $z_a = 0.524$, but also reveal a strong 2175 \AA graphitic dust feature at $z_a = 0.524$. This is the first direct detection of the 2175 \AA feature in a quasar DLA system. We also report on a Keck LRIS spectrum of AO 0235+164 that shows a weak 4428 \AA diffuse interstellar band (DIB) feature at $z_a = 0.524$, the first detection of a DIB feature in a quasar DLA system.

The measured $N(HI)$ from the STIS spectrum and concurrent Asca and previous Asca and ROSAT X-ray spectra are used to find the metallicity in the $z_a = 0.524$ DLA system toward AO 0235+164. These results are compared to a recent determination of the metallicity in this system based on a Chandra X-Ray Observatory ACIS-S spectrum of AO 0235+164 (Turnshek et al. 2003).

This paper is organized as follows. The observations section, §2, describes the spectra that are analyzed. Section §2.1 describes the HST STIS spectra and §2.2 presents the Keck Observatory data. Section §2.3 describes the simultaneous Asca data and spectral fits to all the X-ray data. The analysis section, §3, is divided into four subsections: §3.1, the determination of $N(HI)$ from the DLA line and the spin temperature, §3.2, the metallicity, §3.3, the measurement of dust properties from the 2175 Å feature, and §3.4, the measurement of the DIB feature. The analysis is followed by a discussion section, §4, which covers the implication of these observations regarding the nature of dust and selection effects in DLA systems. This paper concludes with a brief summary, §5.

2. Observations

2.1. HST/STIS Data

AO 0235+164 was observed with HST/STIS on 11 February 1998 (UT) in the spectroscopic mode. The observations consisted of STIS NUV-MAMA G230L (1570–3180 Å), STIS CCD G430L (2900–5700 Å), and STIS CCD G750L (5236–10266 Å) spectra, with total integration times of 12,833 s (5 orbits), 2874 s (1 orbit), and 2160 s (1 orbit) respectively. All of the data were obtained using the 0.5 arcsec wide slit. The data were reduced using STScI STSDAS software. The G750L observation was flat fielded using a contemporaneous flat field exposure to correct fringing. A comparison of the spectrum before and after the fringing correction shows that the corrected spectrum is free from apparent structure due to residual fringing. Before performing a χ^2 analysis on these three spectra, the flux-corrected STIS G230L spectrum was adjusted by multiplication by 0.98 to match the G430L spectrum where the spectra overlap.

2.2. Keck Data

Observations of AO 0235+164 from the Keck Observatory were obtained as part of a program to study the galaxies near AO 0235+164 (P.I. E. M. Burbidge). The observations were obtained on 1997 November 7 (UT) with the Keck II 10 m telescope and the LRIS low

resolution spectrograph. A 300 g/mm 5000 Å blaze grating provided a wavelength coverage of 4000 Å to 9000 Å (with order overlap) and a resolution (with a 1.0 arcsec wide slit) of about 10 Å FWHM and 2.5 Å per pixel sampling. The spectrum of AO 0235+164 discussed in this paper is from an 1800 s integration at a slit PA = 0 degrees that was chosen to include AO, a faint galaxy due north of AO, and object A. The integration begun at HA = 1:05 East and the beginning airmass was 1.02. The data were reduced using VISTA.

Figure 1 shows the HST STIS and Keck LRIS spectra. The 1.0 arcsec wide slit Keck LRIS observation of AO 0235+164 was scaled by 1.58, the ratio of fluxes between an 8.7 arcsec wide and 1.0 arcsec wide slit observation of Feige 110, the standard star observed at the beginning of night. Because slit losses can vary depending on guiding and seeing, the absolute flux of the 7 November 1997 Keck spectrum of AO 0235+164 has a large uncertainty, of order $\pm 20\%$. The Keck observations during the short, half night, program were intended to measure emission lines in faint nearby galaxies, especially [O II] $\lambda 3727$ at $z_e = 0.524$, and were not particularly well suited for high signal-to-noise spectra of AO itself. The Keck spectrum of AO 0235+164 shows structure in the 7000 to 9000 Å range due to less than perfect fringe correction and residuals from atmospheric absorption bands at about 6900 Å and 7600 Å. A comparison of the STIS and Keck spectra scaled to match each other around 6000 Å shows that the Keck spectrum is somewhat steeper than the HST STIS spectrum below 7000 Å. The difference is marginally significant since it amounts to $\pm 5\%$, which is about the maximum uncertainty that is expected in the relative flux calibration for the Keck LRIS spectrum. At wavelengths longer than 7000 Å the Keck spectrum is not reliably flux calibrated due to order overlap. The highly variable AO 0235+164 was about a factor of 2 brighter on 11 February 1998 during the STIS observations than on 7 November 1997, some 4 months earlier.

2.3. Asca Data and Spectral Fitting

Asca observation of AO 0235+164 started on February 11, 1998 at 7:58 UT. The observation lasted for about 16 hours, and yielded about 15 ks of useful data. The data were reduced in a standard manner, where the screening criteria were the same as those used in the reduction of the 1994 Asca data for this object by Madejski et al. (1996). In our analysis, we used the data reduction tools provided by HEASARC; the most recent tools available as of January 1, 2003. This includes the standard response matrices for GIS detectors, and matrices derived from standard calibration files via the `sisrmg` tool for the SIS detectors. The effective area files were calculated using the `ascaarf` tool v. 3.10 using the standard Asca calibration files. All reduction of the SIS data was performed in the BRIGHT2 mode.

For further analysis, the data were binned such that there were at least 20 counts in each new energy bin, and the energy range for spectral fits was restricted to the bandpass of 0.5 - 10 keV for all four instruments. For all four detectors, the background was extracted from the same image as the source, avoiding any obvious point sources. The background-subtracted source count rates were respectively 0.109 ± 0.003 , 0.089 ± 0.003 , 0.065 ± 0.002 and 0.084 ± 0.002 counts s^{-1} in SIS0, SIS1, GIS2, and GIS3 detectors. We saw no measurable variability of the count rate within the span of our observation. Note that those count rates were roughly 2.5 times greater than the count rates during the 1994 Asca observation.

The spectral fitting of the data was entirely analogous to that reported in Madejski et al. (1996): data from all four detectors were fitted to a single common model, including a power law continuum, modified by photoelectric absorption. In agreement with the previous spectra, the inferred column was in excess of the Galactic value. We fixed the Galactic column to 7.6×10^{20} cm^{-2} (Elvis, Lockman, and Wills 1989), and assumed that the excess would be due to the intervening system at $z = 0.524$. For the purpose of comparison with the previous Asca data sets, we assumed (incorrectly, as we argue below) that the entire excess absorption (beyond the Galactic value) is at $z = 0.524$ and obeys solar abundances. With this, the equivalent hydrogen column density at $z = 0.524$ was fitted to be $3.4 \pm 1.1 \times 10^{21}$ cm^{-2} , which, within errors, was consistent with the values measured via previous Asca and ROSAT observations. The energy power-law index α was 0.72 ± 0.07 and the χ^2 for the 1998 Asca data was 260 for 263 PHA bins. This indicates that the spectrum was harder in 1998 than in 1994 when α was 0.93 ± 0.07 , but this was not surprising, as the indices already differed between the previous Asca and ROSAT observations, conducted ~ 5 months apart. As mentioned above, the source was brighter than in the 1994 Asca observation: the 2 - 10 keV model flux for the Feb. 1998 data was 4.1×10^{-12} erg cm^{-2} s^{-1} , vs. 1.2×10^{-12} erg cm^{-2} s^{-1} in Feb. 1994. Figure 2 shows the 1998 Asca X-ray spectrum of AO 0235-164.

Since the absorption values inferred from the ROSAT and the two Asca data sets were consistent with a single value, in our subsequent analysis we fitted all three data sets simultaneously, assuming constant effect of the combined absorption. We assumed that the intrinsic spectrum of the BL Lac object is a simple power law, but we allowed the normalization and the power law index to vary from one data set to another to account for the observed continuum variability. We used the ROSAT and 1994 Asca data reduced in a manner given in Madejski et al. (1996). In addition, we performed the analysis using the current calibration files for Asca and ROSAT, but there was no discernible difference between the two analyses. As above, we fixed the Galactic absorption at 7.6×10^{20} cm^{-2} . Regarding the modeling of the intervening absorption, we followed the approach of Madejski et al. (1996), where we assumed that the absorption at $z = 0.524$ consists of two components, both parameterized via equivalent hydrogen column density. One component, having the primordial composi-

tion of elements, consists of pure hydrogen plus 76 % of the solar abundance value of helium (by number of atoms). The other component represents all processed elements with their relative ratios to each other at the solar value, but it contains no hydrogen, and only 24 % of the solar abundance value of helium. Such an approach is necessary, since the helium in the primordial absorber has an effect on the absorption even in the Asca band. It also allows us to immediately estimate the metallicity of the intervening absorber since the ratio of the processed column to the column inferred from the damped Ly α analysis yields the metallicity of the intervening system in solar units.

Given the modest energy resolution of the Asca or ROSAT detectors, no discrete spectral features were detected in any data sets. With this, the relative contributions of either absorption component are highly correlated, and this is clearly illustrated in Figure 3. While the best-fit values of the primordial and processed columns would be respectively $10.5 \times 10^{21} \text{ cm}^{-2}$ and $2.3 \times 10^{21} \text{ cm}^{-2}$, yielding χ^2 of 528.5 for 535 PHA bins, fixing the primordial column at $5 \times 10^{21} \text{ cm}^{-2}$ (based on the DLA fit – see §3.1) increases χ^2 only to 530.0, and implies that the column density of the processed material is $3.6 \pm 0.8 \times 10^{21} \text{ cm}^{-2}$. With this, we immediately find the metallicity of the intervening system, Z , to be $3.6/5 = 0.72 \pm 0.24$ solar (the quoted uncertainty includes the range of X-ray measurements and the uncertainty of the H I column based on the STIS spectrum, added in quadrature).

3. Analysis

3.1. H I Column Density and Spin Temperature

Figure 4 shows the STIS NUV MAMA G230L spectrum of AO 0235+164 in the region around the DLA line at $z_a = 0.524$ and a χ^2 fit to G230L spectrum from 1690 Å to 2240 Å. This fit gives $N(HI) = 5 \pm 1 \times 10^{21} \text{ cm}^{-2}$. The one σ uncertainty includes both the formal error and an estimate of some of the systematic uncertainties. The one σ formal error in $N(HI)$ from the χ^2 fit and the associated curvature matrix is $(+0.6, -0.5) \times 10^{21} \text{ cm}^{-2}$. The continuum level, continuum slope, and $E(B - V)$ at $z = 0.0$ were left as free parameters in this χ^2 fit so the uncertainties in these values entered the $N(HI)$ formal uncertainty in the proper way from the cross terms in the curvature matrix. Possible systematic errors result from the unknown shape of the local continuum. The continuum may deviate from a power law, and there are uncertainties in the shape of the $z_a = 0$ and $z_a = 0.524$ dust absorption extinction curves. Weak metal lines in the $z_a = 0.524$ and $z_a = 0.852$ absorption systems occur in the wings of the DLA profile along with possible Ly α forest contamination with some uncertainty in the relative line strengths. These systematic errors were investigated by repeating the fitting process assuming different shapes for the continuum and different line

strengths for the weak lines. The relative strengths of all the weak lines are not completely arbitrary. Each line, modeled as a Voigt profile with a single component, has a strength determined by the column density of the ion producing the line. Solar abundances were sometimes used as a guide to determine ranges for column density ratios between selected ions. For example, the Si II column density is constrained to be less than the C II column density in the model for the absorption lines produced by the $z_a = 0.524$ DLA system. Some lines, such as those from Si II, are constrained by multiple lines from Si II within this spectral range. Other absorption lines, including the lines that are Ly α forest lines, are only constrained by the data. Repeating the χ^2 fit after excluding from the model spectrum all the weak lines that are not well detected, and treating all of the observed structure on the wings of the DLA line as noise, results in a higher $N(HI)$ estimate; $N(HI) = 7 \times 10^{21} \text{ cm}^{-2}$. But this model spectrum does not fit the core of the observed DLA line as well as the $N(HI) = 5 \times 10^{21} \text{ cm}^{-2}$ model. Trials with different parameters for the weak metal lines and different values of $R_V = A_V/E(B - V)$ at $z = 0$ and $z = 0.524$ lead to a final estimate of $N(HI) = 5 \pm 1 \times 10^{21} \text{ cm}^{-2}$.

The best fit value for Galactic reddening, $E(B - V)$ at $z = 0.0$, from the fit shown in Figure 4, is $E(B - V) = 0.13$. The Galactic 21 cm H I emission data give $N(HI) = 7.6 \times 10^{20} \text{ cm}^{-2}$ in the direction of AO 0235+164 (Elvis, Lockman, and Wills 1989). Using the average Galactic $N(HI)$ to $E(B - V)$ relationship from Diplaz and Savage (1994), $N(HI) = 4.93 \times 10^{21} \text{ cm}^{-2} E(B - V)$, gives $E(B - V) = 0.154$, very close to the $E(B - V) = 0.13$ from the χ^2 fit used to find $N(HI)$. Repeated trials with different continuum assumptions show that the best fit $E(B - V)$ value at $z = 0.0$ is not well determined from the data because the 2175 Å dust feature at $z = 0.0$ is relatively shallow, the unreddened continuum slope is not known, and the statistical errors in the STIS NUV spectrum of AO 0235+164 at the bluest wavelengths are large. In χ^2 fits to measure the 2175 Å dust feature at $z_a = 0.524$, described in the next section, the $E(B - V)$ at $z = 0.0$ was fixed at $E(B - V) = 0.154$. Setting $E(B - V) = 0.154$ at $z = 0$ in the above fit gives a $\log N(HI) = 21.72$ ($5.2 \times 10^{21} \text{ cm}^{-2}$) at $z_a = 0.524$ which is only 0.02 dex higher than the value above, and within the formal 1σ errors.

Combining the DLA determined $N(HI)$ value with the H I 21 cm absorption observation from Roberts et al. (1976) who found $N(HI) = 2.3 \times 10^{19} T_s \text{ cm}^{-2}$ gives $T_s = 220 \pm 60$ K. The Roberts et al. result assumes complete covering of the background source and is an integration over the entire observed 21 cm feature with the same T_s assumed for all the absorption components. For comparison, T_s has been estimated in a few DLA systems (e.g. Briggs 1987; Cohen et al. 1994) and the range of values is $T_s = 600$ K to $T_s = 1500$ K. There are several uncertainties in deriving T_s from spectroscopic DLA measurements and radio 21 cm absorption. The background radio source and optical/UV source do not coincide

for many quasars (e.g. Briggs 1999). In the case of the $z_a = 0.524$ DLA system toward AO 0235+164, the background radio source is very compact. Thus the T_s estimate for the AO 0235+164 $z_a = 0.524$ DLA system may be somewhat more robust than the T_s estimates in some other DLA systems. However there is an added uncertainty for AO 0235+164 because the $z_a = 0.524$ H I 21 cm absorption is time variable (Wolfe, Davis, and Briggs 1982). An inspection of the 14 epochs of H I 21 cm absorption displayed by Wolfe, Davis, and Briggs (1982), obtained over a four year period from 1977 to 1981, shows that, although there are large (up to a factor of two) changes in individual components, the added uncertainty to T_s due to variability is not large, $\leq 20\%$ peak to peak, if the 21 cm absorption stays within the range observed by Wolfe, Davis, and Briggs (1982). Other systematic errors in T_s are more difficult to estimate and the ± 60 K uncertainty given above reflects only the error in $N(HI)$ combined in quadrature with $\pm 20\%$ as a rough estimate for the effects of variability.

3.2. Metallicity

As discussed above in §2.3, the total metallicity in the $z_a = 0.524$ DLA system can be estimated from the observed $N(HI)$ and X-ray absorption. The main elements contributing to the X-ray absorption in the ROSAT / Asca bands at the column inferred here are oxygen, and to a lesser extent, carbon and iron. The X-ray absorption measurement is particularly valuable, as the inferred column includes a contribution of all phases of the the absorber, not just the gas phase. The observed $N(HI) = 5 \times 10^{21} \text{ cm}^{-2}$ from the DLA fixes the hydrogen column in the “primordial” component. With a fixed “primordial” component, the spectral fit to the X-ray data above gives a metallicity $Z = 0.72 \pm 0.24 Z_\odot$, where again, the range of allowed X-ray absorption and the uncertainty in $N(HI)$ are added in quadrature. There is some added uncertainty due to the time variable nature of the absorber given our use of X-ray data which are at least in part, non-simultaneous with the STIS data. Adding in a 20% additional uncertainty due to variability (a rough estimate based on the maximum range of 21-cm variability observed by Wolfe, Davis, and Briggs (1982) – see above) increases the uncertainty to ± 0.28 . So our final metallicity is $Z = 0.72 \pm 0.28 Z_\odot$.

It is interesting to juxtapose the comparison of the H I absorption data and the X-ray column for AO 0235+164 against those measured in another DLA system at slightly lower redshift, $z_{abs} = 0.312$, located in front of PKS 1127-145 (which is at $z_{em} = 1.187$). This system shows an H I column of $5.1 \pm 0.9 \times 10^{21} \text{ cm}^{-2}$, quite similar to the column in AO 0235+164. Chandra observations of this object revealed excess X-ray absorption above the expected Galactic value (Bechtold et al. 2001). However, this excess is significantly smaller than in AO 0235+164, indicating that the metallicity is less than $0.17 Z_\odot$, much lower than

in AO 0235+164. This implies that the metallicity of the ISM varies significantly from one galaxy to another. We also note that the measurements in both cases are performed in a single line-of-sight, covering at most a patch corresponding to a square parsec of the intervening system, and the ISM of any given galaxy might well show variation of metallicity from one line-of-sight to another.

AO 0235+164 has also been observed with the Chandra X-ray Observatory (Turnshek et al. 2003) to determine the metallicity in the $z_a = 0.524$ DLA system. Turnshek et al. (2003) use the HST STIS spectrum discussed in this paper to obtain an H I column density and they find $N(HI) = 4.5 \times 10^{21} \text{ cm}^{-2} \pm 0.4 \times 10^{21} \text{ cm}^{-2}$. As in this paper, the observed X-ray spectrum is assumed to be a power law with absorption at $z_a = 0$ and $z_a = 0.524$. Turnshek et al. (2003) find a metallicity of $Z = 0.24 \pm 0.06Z_\odot$ using a solar metallicity model for the Galactic absorption and solar abundance ratios for the metals in the absorber at $z_a = 0.524$. Turnshek et al. (2003) also give metallicities assuming a Galactic ISM with no metals and with reduced metals from solar and assuming that the absorber at $z_a = 0.524$ has enhanced α process metals by a factor of 2.5 relative to solar. The six metallicity values found by Turnshek et al. (2003) for the AO 0235+164 $z_a = 0.524$ DLA system, depending on the assumptions, range from $Z = 0.11 \pm 0.03Z_\odot$ to $Z = 0.61 \pm 0.07Z_\odot$. The Turnshek et al. (2003) solar metallicity model at $z_a = 0.524$ and solar metallicities for the Galactic ISM are similar to the assumptions used in this paper. We find $Z = 0.72 \pm 0.28Z_\odot$ using these assumptions and the combined ROSAT / Asca data sets; a metallicity that is 3 times as large as the Turnshek et al. (2003) value of $Z = 0.24 \pm 0.06Z_\odot$. The formal difference between the metallicity found in this paper and that found by Turnshek et al. (2003) is about 2.0σ for the quoted uncertainties before we add the systematic effect due to possible time variability. The effect of the slightly different input values for $N(HI)$ is only 10% and using the value found in this paper, $N(HI) = 5 \times 10^{21} \text{ cm}^{-2}$, would decrease the metallicity of Turnshek et al. (2003) by 10%. The Galactic column density toward AO 0235+164 used by Turnshek et al. (2003) is $N(HI) = 8.7 \times 10^{20} \text{ cm}^{-2}$ (based on 21 cm maps) compared to the column density used in this paper of $N(HI) = 7.6 \times 10^{20} \text{ cm}^{-2}$ (based on a pointed 21 cm observation toward AO 0235+164 - Elvis, Lockman, and Wills (1989)). Given the nature of the 21 cm observations to determine the Galactic $N(HI)$ values and the quoted errors in the 21 cm H I column densities, either value of Galactic column density is possible. The higher value Galactic column used by Turnshek et al. (2003) would tend to give a somewhat lower total absorption at $z_a = 0.524$. Most of the difference in the metallicities between the Asca and ROSAT X-ray data analyzed in this paper and the Chandra X-ray data analyzed by Turnshek et al. (2003) is probably due to different realizations of the noise in the X-ray data sets or due to time variability or some combination of the two effects. Additional differences may result if a single power law is not an accurate representation of the unabsorbed X-ray

spectrum of AO 0235+164. Future X-ray observations that have higher signal-to-noise and resolve some absorption feature or edge will allow more accurate models for the absorption at $z_a = 0.0$ and $z_a = 0.524$ toward AO 0235+164.

Turnshek et al. (2003) also analyze two other DLA systems using Chandra X-ray Observatory data. One of the systems, the DLA at $z_a = 0.313$ toward PKS 1127–145, was analyzed by Bechtold et al. (2001) as discussed above. Turnshek et al. (2003) find as did Bechtold et al. (2001) that only an upper limit to the metallicity can be established for this DLA system although the details of the analysis are different. Turnshek et al. (2003) conclude that there is no evidence for a relatively high metallicity in the PKS 1127–145 DLA system. But they also find that even a zero-metallicity DLA model does not fit the observed X-ray spectrum well so the metallicity is not well determined. Turnshek et al. (2003) find that the $z_a = 0.394$ DLA system toward S4 0248+430 could be metal enhanced with an enhancement similar to the metallicity found in the $z_a = 0.524$ system toward AO 0235+164. But as noted by Turnshek et al. (2003), the S4 0248+430 line of sight could have another high column density absorber at $z_a = 0.051$ which could provide substantial X-ray absorption. The likelihood that the $z_a = 0.051$ is a DLA system is high because the spectrum of S4 0248+430 shows extremely strong Ca II and Na I absorption at $z_a = 0.051$ (Womble et al. 1990). The $N(HI)$ column at $z_a = 0.394$ toward S4 0248+430, as discussed in Turnshek et al. (2003), is based not on a DLA measurement, but on H I 21 cm observations and an assumed spin temperature which increases the uncertainty in the metallicity. The $z_a = 0.524$ DLA system toward AO 0235+164 provides the most certain metallicity measurement of the three DLA systems considered by Turnshek et al. (2003). The other two DLA systems suggest that there is quite a range of metallicity in the low redshift DLA systems.

3.3. The 2175 Å Dust Feature, Dust-to-Gas, and Dust-to-Metals

The continuum spectrum of AO 0235+164 (Figure 1) shows a strong, broad absorption feature centered at about 3300 Å (observed), near the expected wavelength of the 2175 Å dust feature at $z_a = 0.524$. In order to analyze this feature, it is necessary to model the underlying spectrum of AO 0235+164 and to have a numerical model for dust extinction. The underlying spectrum of AO 0235+164 is assumed to be a power-law continuum (or several power-laws connected at “break-point” wavelengths). The numerical model includes narrow absorption features in the UV (since these were necessary for the DLA analysis). Narrow gaps in wavelength are excluded from the fit at the locations of absorption features in the optical spectrum. The dust extinction is modeled using the extinction formulae from Cardelli, Clayton, and Mathis (1989, hereafter CCM) for Galactic dust and the extinction

formulae from Pei (1992) for LMC dust, SMC dust, and a modified Galactic version (see below). The advantage of the CCM formulae is that a larger range of Galactic extinction curves can be fit using $R_V = A_V / E(B - V)$ as a variable as well as $E(B - V)$. The Pei (1992) extinction formulae fix R_V at 3.1 for Galactic extinction (the most common value found). A summary of the fits to the spectrum of AO 0235+164 including dust extinction is given in Table 1. Figure 5 shows the continua from three χ^2 fits to the AO 0235+164 spectrum over the spectral region from 2500 Å to 8700 Å. To emphasize the continuum features, only the continua are plotted above the spectrum (i.e. no absorption features are plotted above the spectrum). The fits shown are for models with Galactic, LMC, and SMC type dust (fits 1, 2, and 3 respectively in Table 1). Overlaid on the observed spectrum of AO 0235+164 in Figure 5 is the Galactic dust model. The Galactic dust model is the best fit of the three shown.

Multiple dust components are included in all of the fits, one at $z_a = 0$ and one or more at $z_a = 0.524$. The $z_a = 0$ Galactic absorption is fixed, for all the models listed in Table 1, with $E(B - V) = 0.154$ (based on the H I 21 cm as described above) and $R_V = A_V / E(B - V) = 3.1$. The CCM formulae are used to model the dust at $z_a = 0.0$. As described in the previous section, the $E(B - V)$ at $z = 0.0$ is not well determined by these spectra. A range for the $z_a = 0.0$ dust extinction can be estimated by varying $E(B - V)$ and comparing, by eye, the depth of the resulting 2175 Å feature to the observed data. The range of values found is from $E(B - V) = 0.12$ to $E(B - V) = 0.19$ and this range is used later to estimate part of the systematic errors in the parameters to fit 1 (Table 1) which is our best estimate for the dust parameters at $z_a = 0.524$ along the AO 0235+164 line-of-sight.

Galactic type dust extinction at $z_a = 0.524$ produces the best fit to the AO 0235+164 spectrum when comparing Galactic, SMC, and LMC type dust. The observed spectrum does not fit the CCM extinction function perfectly: systematic deviations can be seen at $\lambda > 8700$ Å, at $\lambda < 2500$ Å, and on the red half of the $z_a = 0.524$ 2175 Å feature (Figure 5). The Galactic 2175 Å feature varies in shape from line-of-sight to line-of-sight (e.g. Fitzpatrick and Massa 1986), so small deviations around 2175 Å at $z_a = 0.524$ are not surprising. The best fit parameters from fit 1 (Galactic dust) are $E(B - V) = 0.227 \pm 0.003$ and $R_V = 2.51 \pm 0.03$. The above errors are only the formal errors in the χ^2 fits. We can estimate that part of the systematic error due to uncertainties in the $z_a = 0.0$ extinction by using the above mentioned range of $E(B - V) = 0.12$ to $E(B - V) = 0.19$ at $z_a = 0.0$. Re-fitting the observations with these values gives $E(B - V) = 0.23 \pm 0.01$ and $R_V = 2.5 \pm 0.2$ at $z_a = 0.524$. Other systematic errors are likely because the extinction at $z_a = 0.524$ is not a perfect match to “typical” Galactic extinction and does deviate significantly in the far-UV. The best fit background source power law over 2500 Å to 8700 Å has $\alpha = -1.75 \pm 0.01$ (formal error) for $f_\nu \propto \nu^\alpha$. The systematic error due to the uncertain $z_a = 0.0$ extinction

increases the error and gives $\alpha = -1.75 \pm 0.15$. The above formal errors from the χ^2 fits and those listed in Table 1 are probably severe underestimates of the true errors but they are an indication of what the statistical errors would be if the shape of the extinction curve at $z_a = 0.524$ and the extinction parameters at $z_a = 0.0$ were known accurately.

The extinction curves for the SMC and LMC differ greatly from the extinction curves typically observed in the Galaxy. The LMC extinction curve has a less pronounced 2175 Å absorption feature compared to the Galaxy for lines-of-sight with similar total A_V . The SMC extinction curve has practically no 2175 Å graphite feature. Figure 5 shows χ^2 fits to the observed AO 0235+164 spectrum using the SMC and LMC extinction curves from Pei (1992) at $z_a = 0.524$. As expected, the SMC type extinction does not fit the observations. The LMC extinction model for the $z_a = 0.524$ system cannot fit the observations over the 2500 Å to 8700 Å spectral region because the predicted UV extinction is too strong when the model 2175 Å feature has the same depth as the observed feature. The best χ^2 fit misses both in the continuum and in the depth of the 2175 Å feature. In order to further explore the possibility of fitting the AO 0235+164 spectrum using an LMC type extinction curve, a model (fit 4 in Table 1) was found that reproduces the 2175 Å feature reasonably well. But this model, that only fits the spectrum over the a restricted wavelength range from 2800 Å to 6000 Å, has a number of unusual features. The underlying spectrum is found to rise in units of νf_ν and the total extinction at 2500 Å (observed) is more than a factor of 100 compared to a factor of 16 for the Galactic extinction model. The unabsorbed underlying flux of $\sim 3 \times 10^{-14}$ erg cm $^{-2}$ s $^{-1}$ at ~ 2500 Å (at the time of these observations) - would make the de-reddened AO 0235+164 a very unusual BL Lac object relative to other strongly beamed and presumably less extinguished BL Lac objects. A simpler explanation is that the extinction in the $z_a = 0.524$ DLA system is more similar to Galactic extinction than LMC extinction.

In order to examine the possibility of a less restrictive dust model, a fit to the observations was made using a “stacked” absorber model at $z_a = 0.524$. One component consisted of a Galactic absorber and the other an LMC type absorber. This fit is listed as number 6 in Table 1. The result of the χ^2 fit was to minimize the LMC component ($E(B - V) \leq 0.005$). This shows that mixing LMC and Galactic type absorption does not improve the fit to this absorption system. A complete investigation of the kinds of extinction laws allowed by these data is beyond the scope of this paper. But amongst the Galactic, LMC, and SMC type extinction models, the Galactic type absorption fits the data the best. Galactic type absorption does fail to match the data below 2500 Å (observed), but this failure in the far-UV cannot be fixed by adding SMC or LMC type absorption to create a multi-component absorber.

The most significant fractional deviations in Figure 5 between the observed spectrum and the Galactic extinction model for the $z_a = 0.524$ system occur at $\lambda \leq 2500$ Å. Attempts

to fit a more complete wavelength region, from 1690 Å to 8700 Å, using a single power law and variable Galactic absorption at $z_a = 0.524$ result in a fit similar to that shown in Figure 5. The furthest UV part clearly does not match the model spectrum and the χ^2 fitting process does not give the far-UV points much weight because the S/N there is lower relative to the S/N further to the red. This relatively strong observed far-UV spectrum (below about 2500 Å observed) can result from either an intrinsic AO 0235+164 spectrum ($z_e = 0.94$) that rises to the blue above the best fit power law or from an extinction curve at $z_a = 0.524$ that has less UV extinction than the CCM Galactic model. Galactic extinction is known to vary from one line-of-sight to another particularly in the far-UV, presumably because the number of very small particles relative to other dust particles is highly non-uniform (e.g. Fitzpatrick 1999). Using the Pei (1992) model for Galactic extinction and reducing the coefficient for the far-UV extinction (to 0.73 of the Pei value) produces a better fit to the overall spectrum (from 1690 Å to 8700 Å observed). This model is listed as fit 5 in Table 1. However, this model does not match the data in detail (i.e. at $\leq 5\%$ fractional variations everywhere). A better match to the observed spectrum can be obtained by using two power laws with $f_\nu \propto \nu^{-1.75}$ at $\lambda > 2549$ Å and $f_\nu \propto \nu^{+0.28}$ at $\lambda < 2549$ Å (observed). This model is listed as fit 7 in Table 1. A steeply rising underlying spectrum to shorter wavelengths would miss the observed X-ray spectrum unless there is a further inflection at wavelengths between the observable optical-UV and X-ray spectral regions. A complicated underlying spectrum with four power-law components or two power-law components plus a “bump” cannot be ruled out by the data. A Galactic type extinction curve can describe the $z_a = 0.524$ system, but it requires somewhat less than normal far-UV ($\lambda_{rest} < 1700$ Å) extinction and minor deviations from the CCM extinction shape: this can fit the observation, and be consistent with an underlying spectrum with one UV-optical power-law and one X-ray power-law component. Without additional assumptions or constraints, it is not possible to determine conclusively both the underlying spectral shape and the extinction curve. For the remainder of the paper, we will primarily discuss the data in terms of the Galactic extinction model at $z_a = 0.524$ with less far-UV extinction and a single power law intrinsic spectrum in the optical-UV spectral region. But other combinations of extinction and underlying spectra can provide possible fits to these observations.

The dust-to-gas ratio for DLA systems is often given by a dimensionless parameter k which is a ratio between dust optical depth and $N(HI)$ defined by $k \equiv 10^{21}(\tau_B/N(HI))$ cm⁻² (Pei 1992). Using $E(B - V) = 0.23 \pm 0.01$, $R_V = 2.5 \pm 0.2$, and $N(HI) = 5 \pm 1 \times 10^{21}$ gives $\tau_B = 0.74$ and $k = 0.15 \pm 0.03$. The value of $k = 0.15 \pm 0.03$ is 0.19 ± 0.04 of the average Galactic value of $k = 0.78$ and similar to $k = 0.16$ for the LMC (Pei 1992). The observed $E(B - V)$ vs. $N(HI)$ correlations for the Galaxy, the LMC, and the SMC show considerable scatter from line-of-sight to line-of-sight, but the AO 0235+164 $z_a = 0.524$

$N(HI)$ and $E(B - V)$ point is typical of the LMC values and well outside the scattered Galactic values (Pei 1992). Using the metallicity estimate from the previous section gives a dust-to-metals ratio, k/Z , of 0.27 ± 0.12 of $(k/Z)_{Galactic}$. For d_m , the dust-to-metals mass ratio, assuming $d_m(AO) = 0.27 \times d_m(GAL)$, $d_m(GAL) = 0.51$ (Pei, Fall, and Hauser 1999), gives $d_m(AO) = 0.14 \pm 0.06$. Assuming that $d_m(AO)$ scales from the Galactic as $(k/Z)_{AO}/(k/Z)_{Galactic}$ implies that the density of dust grains is the same in the AO $z_a = 0.524$ system as it is in the Galaxy. This assumption depends on the mix of grains because silicate and graphite grains have different densities. With $d_m(AO) = 0.14$, the $z_a = 0.524$ DLA system has converted less metals to grains compared to the Galaxy, LMC, or SMC which have d_m values of 0.51, 0.36, and 0.46 respectively. Averaged over all objects as a function of redshift, d_m , the global dust-to-metals mass ratio, relates the comoving density of interstellar dust Ω_d to the comoving density of heavy elements Ω_m (all in units of the closure density) via $\Omega_d = d_m \Omega_m = d_m Z \Omega_g$ (Pei, Fall, and Hauser 1999).

3.4. Diffuse Interstellar Bands

The shortest wavelength and strongest of the known DIBs at 4428 Å (rest) appears in the Keck LRIS spectrum of AO 0235+164 at the expected wavelength, $\lambda_{obs} = 6747$ Å, for $z_a = 0.524$ (Figure 6). The central depth, A_c , of the observed feature is 0.040 ± 0.005 , the equivalent width is $1.13 \text{ Å} \pm 0.04 \text{ Å}$ (observed), and the width is about 32 Å FWHM (observed). The Keck LRIS spectrum is noisier further to the red due to incomplete correction for fringing, and thus the other DIBs are not cleanly detected but there is a depression at the predicted position of the 4882 Å DIB. The $z_a = 0.524$ 4428 Å DIB also appears in the STIS CCD G750L spectrum (Figure 1) at lower signal-to-noise. The 4428 Å DIB parameters for HD 183143, a line-of-sight commonly used for Galactic DIB comparisons, are $W_\lambda = 3.4 \text{ Å}$, $A_c = 0.15$, and FWHM = 18 Å (Herbig 1995). A comparison to the observed 4428 Å DIB parameters at $z_a = 0.524$ gives in rest units $W_\lambda(AO) / W_\lambda(HD) = 0.22$, $A_c(AO)/A_c(HD) = 0.26$, and FWHM(AO) / FWHM(HD) = 1.2. The strength of the AO 0235+164 4428 Å DIB is about 0.25 of the DIB observed toward HD 183143 and the other, weaker DIBs are expected to roughly scale by this factor of 0.25 in both central depth and W_λ (e.g. Herbig 1995).

The presence of the DIBs in stellar spectra is correlated with reddening by dust. The central depth, A_c , of the 4428 Å DIB feature is roughly proportional to $E(B - V)$ in the Milky Way. For a sample of Perseus OB1 stars, Krelowski et al. (1987) find $A_c = 0.0117 + 0.0788 E(B - V)$ (where A_c is expressed in fractional units). For the observed $E(B - V) = 0.23 \pm 0.01$ in the $z_a = 0.524$ AO 0235+164 system, the above equation gives a predicted A_c

$= 0.030 \pm 0.002$. The observed A_c is 0.040 with errors of about ± 0.005 . Given the errors in the observed A_c and $E(B - V)$ and the known scatter in the Galactic $E(B - V) - A_c$ correlation (Krelowski et al. 1987), the DIB strength to reddening ratio in the $z_a = 0.524$ DLA system is similar to the ratios found along Galactic lines-of-sight.

4. Discussion

The $z_a = 0.524$ absorber toward AO 0235+164 shows dust absorption with a 2175 Å feature similar to that seen in the Galaxy. The Galactic type extinction curves form roughly a one parameter family parameterized by R_V (CCM) with a range of observed values $2.2 \leq R_V \leq 5.8$. The best fit to the $z_a = 0.524$ extinction curve has $R_V = 2.5 \pm 0.2$, but the most common value of R_V in the Galaxy, $R_V = 3.1$ cannot be ruled out. Fixing R_V at 3.1 at $z_a = 0.524$ and refitting the observations produces a qualitatively similar fit to that shown in Figure 5. Although formally a less acceptable fit, given the unknown nature of the deviations between the fit and the observations in the 1700 Å to 2500 Å (observed) wavelength region, it is reasonable to accept qualitatively similar extinction curves. At values of $R_V \geq 4.0$, the CCM Galactic extinction curves redshifted to $z_a = 0.524$ become a poor match qualitatively to the observed data.

If the extinction curve at $z_a = 0.524$ were known to be exactly the same as a typical Galactic curve, then it would be possible to deredden the observed spectrum to obtain the underlying BL Lac spectrum. Figure 7 shows the result from dereddening the observed spectrum using the CCM model with $E(B - V) = 0.23$ and $R_V = 2.5$ at $z_a = 0.524$ and $E(B - V) = 0.154$ and $R_V = 3.1$ at $z_a = 0$. These are the parameters from the χ^2 fit described in §3.3 (fit 1 in Table 1). The UV continuum at $\lambda_{obs} \leq 2500$ Å, rises to shorter wavelengths. The slope is steep with $\nu f_\nu \propto \nu^{+1.28}$ (as determined from fitting a two-piece power law with a break at 2549 Å, fit 7 in Table 1). Figure 8 shows the relationship of the dereddened AO 0235+164 spectrum in the optical-UV to the observed and modeled X-ray spectra. The underlying best fit X-ray spectrum does have a positive slope in νf_ν units with $\nu f_\nu \propto \nu^{+0.22 \pm 0.09}$. The spectra of BL Lac objects are thought to be produced by synchrotron emission at low frequencies (in the case of AO 0235+164 this produces the flux in the optical to UV frequency range falling in νf_ν) and a self Compton component at higher frequencies (rising in νf_ν to a cutoff frequency in the γ -ray range). AO 0235+164 would have to have an additional component if the apparent rising flux in the observed wavelength interval $1700 \text{ Å} \leq \lambda_{obs} \leq 2500 \text{ Å}$ were due to the underlying spectrum: we consider this unlikely.

An alternative to explaining the observed spectrum with Galactic type absorption at $z_a = 0.524$ – which would require a relatively complex underlying spectrum – is to allow

for extinction laws outside the “typical” Galactic. As discussed in §3.3, the Pei (1992) parameterization of the Galactic extinction law can be modified to produce less far-UV extinction by reducing the value of the coefficient of that component. It is not clear that this produces a physically reasonable extinction curve; besides, the extinction curve that is produced does not fit the observed flux in detail under an assumption that the underlying flux is a single power-law component. However, given the fact that the standard Galactic (CCM or Pei 1992) extinction curve does not fit most Galactic observations in detail around the 2175 Å feature and in the far-UV, the observed spectra could result from Galactic type extinction at $z_a = 0.524$ with less absorption in the far-UV band, at $\lambda_{rest} < 1700$ Å. The observed variations in the Galactic extinction in the far-UV (Fitzpatrick 1999) do suggest that the relative number distribution of small grains is an independent parameter in dust extinction. An attempt to invoke an LMC or SMC type extinction curves to explain the extinction at $z_a = 0.524$ does not work because the observed 2175 Å feature is so strong. A completely new kind of extinction curve is also possible, but in that case, there are few constraints on any measurable quantities such as $E(B - V)$ at $z_a = 0.524$, because neither the underlying spectral slope nor the unextincted flux are known.

The absorber responsible for the $z_a = 0.524$ absorption toward AO 0235+164 could be a galaxy about 2 arcsec south (object A) (Smith, Burbidge, and Junkkarinen 1977) or another object (object A1) about 1 arcsec East (Yanny, York, and Gallagher 1989). Object A has a Seyfert 1 galaxy emission line spectrum with strong associated absorption or weak BAL type absorption (Burbidge et al. 1996). Object A1 has [O II] λ 3727 emission at $z_e = 0.524$ based on narrow band imaging with a filter tuned to redshifted λ 3727 at $z = 0.524$ (Yanny, York, and Gallagher 1989). Spectroscopy of object A1 is needed to verify that it is indeed a galaxy at $z = 0.524$, but the [O II] results make that likely. Although the AO 0235+164 – subtracted HST WFPC2 image shown in Burbidge et al. (1996) is noisy, the image suggests that both A and A1 are disk galaxies (Burbidge et al. 1996). With this, the existing imaging, spectroscopy of the nearby objects, and absorption spectra are all consistent with the interpretation that the $z_a = 0.524$ absorption is produced by a line-of-sight through a galaxy disk or pair of galaxy disks. The impact parameter is about $14 h_{65}^{-1}$ kpc for object A and $7 h_{65}^{-1}$ kpc for A1 assuming $\Omega_M = 0.3$, $\Omega_\Lambda = 0.7$ and where $h_{65} = H_0/65$ km s⁻¹ Mpc⁻¹. Therefore, depending on the inclination, the $z_a = 0.524$ DLA system may sample a galaxy disk at a distance from the nucleus which is not too dissimilar to the position of the Sun in the Milky Way. It is also possible that a galaxy-galaxy interaction plays a part in determining the properties of this absorber if A1 is at $z = 0.524$ and interacting with A (Yanny, York, and Gallagher 1989). The 21 cm H I absorption has multiple deep components (Wolfe, Davis, and Briggs 1982) and the observed Mg II absorption has a large total velocity width, 250 km s⁻¹, and shows more components than the 21 cm (Lanzetta and Bowen 1992). The large

range of absorption velocities and the large number of individual absorption components might suggest absorption by an interacting pair rather than absorption by a single isolated disk galaxy. The low value of the dust-to-metals mass ratio d_m for this system, 0.14 vs. 0.51 for the Galaxy, could be produced by the release of metals from dust due to cloud–cloud collisions. If the absorption is primarily produced by gas involved in an interaction between objects A and A1, then the $z_a = 0.524$ system may not be typical of high metallicity DLA disk absorbers.

Object A may produce a DLA absorber that is not typical of DLA absorbers because it has intrinsic absorption and an AGN type mass outflow. Because the geometry and extent of AGN mass outflows in general are not well known, it is possible that a mass outflow could change the characteristics of disk-like gas far from the central source. As mentioned above, the impact parameter between object A and the BL Lac object corresponds to $14 h_{65}^{-1}$ kpc. The observations of object A (Burbidge et al. 1996) are very low resolution and constitute a single epoch so it is not possible to determine if the intrinsic absorber is close to the AGN using partial covering and/or time variability. Other examples of DLA systems associated with AGN are needed to determine if there is any correlation between the AGN properties and the DLA absorption properties in the host galaxies.

The dusty $z_a = 0.524$ DLA system toward AO 0235+164 is an example of the kind of DLA system that will suffer selection effects (Pei and Fall 1995) when the background sources are selected from a magnitude limited sample. The large inferred extinction is shown graphically in Figures 7 and 8 where the dereddened and observed spectra are both plotted. At the observed frame B band, 4400 Å, the extinction due to dust at $z_a = 0.524$ is 1.3 magnitudes ($R_V = 2.5$ and $E(B - V) = 0.23$). The observed apparent number counts of quasars as a function of apparent magnitude, m , can be described as $N(m) \propto 10^{0.4\beta m}$ where $N(m)$ is the number of quasars in units of $\text{deg}^{-2} \text{mag}^{-1}$. For B band counts Pei, Fall, and Hauser (1999) find $\beta = 2.0$. This fairly steep rise in the number of quasars as a function of m holds for $B \leq 20$. Because the number counts are an exponential, the fraction of quasars missed due to dust obscuration is independent of the limiting magnitude of the survey for $B_{lim} \leq 20$. Integrating $N(m)$ with $\beta = 2.0$, the fraction of DLA systems missed due to selection effects is $1 - e^{-1.84A_{B(obs)}}$ where $A_{B(obs)}$ is the extinction of the DLA system at the observed frame B band. Systems similar to the $z_a = 0.524$ absorber, with $A_{B(obs)} = 1.3$, would be underrepresented by a large factor with 91% missing from a B magnitude limited quasar survey. If there were systems like this at a redshift of $z_a = 2.0$, the extinction at 4400 Å (obs) would be about 2.0 magnitudes and about 97% would be missing due to selection effects.

Absorption systems, with $N(HI) \sim 5 \times 10^{21} \text{ cm}^{-2}$, are near the high $N(HI)$ turnover

(high $N(HI)$ knee) in the H I column density distribution (Storrie–Lombardi, Irwin, and McMahon 1996a; Rao and Turnshek 2000). It is important to count such systems accurately in order to measure the evolution with z of the mean contribution of neutral gas to the cosmological mass density, $\langle\Omega_g\rangle$ (Storrie–Lombardi, Irwin, and McMahon 1996b). The observed H I column density distribution for $N(HI)$ below the high $N(HI)$ knee is typically described as a power law with $f(N_H) = f_*N_H^{-\beta}$. Because the observed value of β is around 1.5 – 1.7 (Storrie–Lombardi, Irwin, and McMahon 1996a) and one is integrating $Nf(N)dN$, the highest column density systems, up to the high $N(HI)$ knee, contribute the most to the integrated $N(HI)$ at each redshift. Absorption systems that are missed due to dust can contribute significantly to $N(HI)$ without contributing much added search path thus leading to an underestimate of $\langle\Omega_g\rangle$ which is often estimated from the observed function, $\Omega_{DLA}(z)$, which just includes the DLA contribution.

At low redshift, the observed DLA H I column density distribution shows a relative excess of high column density systems compared to the high redshift H I column density distribution (Rao and Turnshek 2000). Rao and Turnshek find no observed evolution of $\Omega_{DLA}(z)$ with z . Rao and Turnshek (2000) consider the AO 0235+164 $z_a = 0.524$ DLA system to be a biased line-of-sight because it has a 21 cm H I detection, but the 21 cm H I observations of Roberts et al. (1976) were tuned to $z_a = 0.524$ based on the detection of Mg II absorption at that redshift. Thus the $z_a = 0.524$ system could be considered a Mg II selected absorption system and is not a system discovered by 21 cm H I absorption. The OI 363 $z_a = 0.0912$ and $z_a = 0.2212$ absorption systems, both found to have DLA absorption by Rao and Turnshek (1998), also have 21 cm H I absorption (Lane et al. 1998). The OI 363 absorption systems are included in the Rao and Turnshek survey statistics and the AO 0235+164 $z_a = 0.524$ system is not included. The point of the above discussion is that the sample selection criterion used by Rao and Turnshek (2000), namely the exclusion of all previously known 21 cm absorbers, is not a completely robust criterion for rejecting the Mg II selected absorber toward AO 0235+164. The “no known 21 cm systems” rule was used to avoid a bias in favor of high $N(HI)$ systems, but, in a few cases, that rule may produce a bias against high $N(HI)$ systems. Maybe the $z_a = 0.524$ absorber would have made the Rao and Turnshek (2000) sample if nothing were known about the 21 cm absorption or maybe the $z_a = 0.524$ absorber without dust would have made that sample. If the AO 0235+164 $z_a = 0.524$ absorber $N(HI)$ were included with the 16 other DLA systems in Rao and Turnshek, it would increase the total $N(HI)$ in that low z sample by 22% .

Rao and Turnshek (2000) use their low redshift sample of DLA systems to determine the low redshift end of $\Omega_{DLA}(z)$. Their sample is binned into two bins with the lowest redshift bin including objects with redshifts from $z = 0.0$ to 0.8. If AO 0235+164 with $z_a = 0.524$ were to be included in this bin, the total column density in this bin increases by

about 35% while the search interval increases only slightly. The $\log_{10}\Omega_{DLA}(z)$ value in this bin would increase by about 0.13 from -2.65 to -2.52 for the $q_0 = 0.5$ model plotted in Rao and Turnshek (2000). If the inclusion of AO 0235+164 were the only change to the $\Omega_{DLA}(z)$ function illustrated by Rao and Turnshek (2000), the shape of the function would suggest an increasing $\Omega_{DLA}(z)$ to lower redshifts - but the error bars in the values of the binned $\Omega_{DLA}(z)$ are too large make any definite statements. This does illustrate the importance of high $N(HI)$ systems to the determination of $\Omega_{DLA}(z)$, and missing a few such systems due to dust could change the observationally determined evolution of $\Omega_{DLA}(z)$ if dust evolves with redshift.

A number of studies use DLA and dust characteristics to estimate the corrections for selection effects. These studies include Fall and Pei (1993), Pei and Fall (1995), and Pei, Fall, and Hauser (1999). The $z_a = 0.524$ absorption system toward AO 0235+164 has some dust characteristics that differ from the assumed dust properties in Pei and Fall (1995) and Pei, Fall, and Hauser (1999). Pei and Fall (1995) assume that the extinction curve for DLA dust is intermediate between the LMC and SMC extinctions at $\lambda < 2000 \text{ \AA}$ while the $z_a = 0.524$ absorber resembles more closely the Galactic extinction curve, but with possibly less extinction than Galactic at $\lambda < 1700 \text{ \AA}$. The LMC and SMC extinction curves have more extinction at $\lambda < 1700 \text{ \AA}$ than the Galactic extinction curve. The $z_a = 0.524$ system has a low dust to metals ratio k/Z of $0.27 \pm 0.12 (k/Z)_{Galactic}$ while Pei and Fall (1995) and Pei, Fall, and Hauser (1999) assume that dust-to-metals is roughly constant at the Galactic value. A lower dust-to-metals and less UV extinction would produce less correction for dusty DLA systems than the corrections found by Pei and Fall (1995). The observation of one dusty low redshift DLA system with Galactic type dust toward a high apparent brightness, radio selected BL Lac object, a rare type of AGN, suggests that dusty systems with these dust characteristics may be common. The dust extinction in DLAs may be more complex than the model of Pei and Fall (1995) with SMC or LMC type dust typical in low metallicity systems and Galactic type dust common in higher metallicity systems. More dusty DLA systems must be observed before the corrections for DLA systems missed due to dust extinction can be considered accurate.

Corrections for dust are important in the determination of the $N(HI)$ weighted mean metallicity $[\langle Z(z) \rangle]$ in DLA systems. Prantzos and Boissier (2000) calculate a model for absorption by disk systems which shows that the observed lack of metallicity evolution in DLAs (e.g. Pettini et al. 1999) is a result of observational bias effects, in particular the effect of dust extinction in high column density, high metallicity systems. At the current time, because the number of well studied DLA systems is small, the inclusion or exclusion of individual systems with a high metallicity and a high $N(HI)$ can greatly influence the empirically determined $[\langle Z(z) \rangle]$ (Prochaska and Wolfe 2000). Pettini et al. (1999) find for

the lowest redshift bin, $z < 1.5$, that $[\langle \text{Zn}/\text{H} \rangle] = -1.03 \pm 0.23$ (on a logarithmic scale relative to solar). The Pettini et al. (1999) measurement is based on 10 DLAs with $\sum N(\text{HI}) = 7.7 \times 10^{21} \text{ cm}^{-2}$. If the $z_a = 0.524$ system, with $N(\text{HI}) = 5 \pm 1 \times 10^{21} \text{ cm}^{-2}$ and $Z = (0.72 \pm 0.28) Z_\odot$, were included in the bin with $[\text{Zn}/\text{H}] = \log_{10}(0.72) = -0.14$, then the $N(\text{HI})$ weighted average would increase to $[\langle \text{Zn}/\text{H} \rangle] = -0.47$, i.e. the metallicity in this bin would jump from $0.093 Z_\odot$ to $0.34 Z_\odot$.

The AO 0235+164 $z_a = 0.524$ DLA system cannot be included in the sample of Pettini et al. (1997b, 1999): this is because it does not have a metallicity determined from Zn II measurements. The X-ray determined metallicity in the $z_a = 0.524$ system is weighted most heavily to the abundance of oxygen with some contribution from carbon and iron (§3.2). Oxygen and zinc may not reflect the same metallicity so it would be important to measure the Zn II lines in the AO 0235+164 spectrum. The Zn II lines at 2025 Å and 2062 Å will appear at 3086 Å and 3142 Å at $z_a = 0.524$ and, being near the atmospheric cutoff in an AGN with a red observed spectrum, these lines will be difficult to observe. Pettini et al. (1997b) chose Zn as a metallicity indicator because Zn is relatively resistant to depletion onto dust grains. Measurements of metallicity using X-ray absorption are also insensitive to metal depletion onto dust grains. The Zn II based metallicities and the X-ray determined metallicities will differ if the abundances reflect α process enhancements and the X-ray analysis is done assuming no α process enhancement.

Turnshek et al. (2003) consider the evolution of metallicity with redshift using three Chandra X-Ray Observatory determined metallicities (AO 0235+164 $z_a = 0.524$, PKS 1127–145 $z_a = 0.313$, and S4 0248+430 $z_a = 0.394$) combined with the Pettini et al. (1999) Zn II based metallicities. Turnshek et al. (2003) consider the case for solar metallicities and alpha process enhanced metallicities (by a factor of 2.5) in the absorber and find different equivalent Zn II metallicity values in the two cases. As described in §3.2, Turnshek et al. (2003) find a metallicity about one third the value in this paper for the $z_a = 0.524$ DLA toward AO 0235+164 when models with similar assumptions are compared. Turnshek et al. (2003) find that the metallicities for the three DLA systems might provide support for an increasing $[\langle Z(z) \rangle]$ to lower redshifts using the Pettini et al. (1999) Zn based values to determine the high redshift $[\langle Z(z) \rangle]$ points. The higher metallicity value found in this paper would tend to make the evolution of $[\langle Z(z) \rangle]$ toward lower z more pronounced. However, Turnshek et al. (2003) conclude that the trend in the lowest redshift points in their $[\langle Z(z) \rangle]$ analysis depends on the treatment (exclusion or inclusion) of the PKS 1127–145 DLA which has as large an H I column density as the AO 0235+164 DLA and is treated as having zero metallicity. Also Turnshek et al. (2003) find that the lowest redshift value of the $[\langle Z(z) \rangle]$ function depends strongly on the assumption of solar relative abundances versus α process enhanced abundances. The current samples of DLAs are just too small to determine the

low redshift end of $[\langle Z(z) \rangle]$ function because most of the contribution in $N(HI)$ comes from a few extremely high column density systems like the AO 0235+164 DLA. The inclusion or exclusion of a single system can greatly influence the $N(HI)$ weighted quantities like $[\langle Z(z) \rangle]$: in particular the exclusion of the AO 0235+164 DLA. A large change in metallicity due to the inclusion or exclusion of one system points out how fragile the current $[\langle Z(z) \rangle]$ measurement is due to small number statistics. The difference in metallicity found in this paper vs. the values found by Turnshek et al. (2003) are also problematical in determining $[\langle Z(z) \rangle]$. An improved determination can be made using a simultaneous soft X-ray observation and an HST observation to determine $N(HI)$ based on the DLA line. This would reduce the uncertainty due to the possible time variability of the absorption. Unfortunately, AO 0235+164 is often too faint to be economically observed with HST in the UV. A high resolution observation of the Zn II lines at $z_a = 0.524$ would also be very valuable, but difficult due to the atmospheric cutoff and the faintness of the BL Lac object at these wavelengths.

At the present time, the value of $[\langle Z(z) \rangle]$ at low redshift is strongly influenced by the metallicity and by the inclusion or exclusion in the low redshift sample of one system, the $z_a = 0.524$ DLA toward AO 0235+164. AO 0235+164 is now the prototypical line-of-sight substantially reddened by dust extinction due to an intervening DLA system. This illustrates the potential importance of high $N(HI)$ high Z systems that are missed in magnitude limited surveys due to dust extinction. Observations of samples of quasars free from selection effects due to extinction will eventually resolve the issue of missed DLA systems with dust. The CORALS survey (Ellison et al. 2001), which selects background quasars for DLA systems on the basis of radio emission only, has found a relatively small correction (less than a factor of two) to the neutral gas fraction. The question of the metallicity correction due to dust selection effects remains unresolved because the high column density systems such as AO 0235+164 $z_a = 0.524$ are so rare that the number of systems is poorly constrained by the current sample (Ellison et al. 2001).

5. Summary

The properties of the $z_a = 0.524$ absorption system toward AO 0235+164 are intermediate between the high redshift DLAs and the Milky Way Galactic disk. The absorber at $z_a = 0.524$ has many qualitative similarities in absorption to the Galactic disk around the position of our Sun. The spin temperature at $T_s = 220 \pm 60$ K is relatively low compared to other DLAs with 21cm absorption and roughly near the typical value for the Galaxy. There is dust extinction at $z_a = 0.524$ with a 2175 Å feature while other DLAs do not show this feature. The best fit to Galactic extinction over $2500 \text{ Å} \leq \lambda_{obs} \leq 8700 \text{ Å}$ at $z_a = 0.524$

gives $E(B - V) = 0.23 \pm 0.01$ and $R_V = 2.5 \pm 0.2$. The diffuse interstellar bands that are associated with dust are present, and the DIB strength matches that predicted from the Galactic DIB vs. $E(B - V)$ correlation to within about 25%. The metallicity of the system is relatively high compared to most DLA systems, $Z = 0.72 \pm 0.28 Z_\odot$. Although it should be noted that an independent X-ray measurement using a Chandra X-ray Observatory ASIS-S spectrum gave (with similar assumptions) $Z = 0.24 \pm 0.06 Z_\odot$ for the $z_a = 0.524$ system toward AO 0235+164 (Turnshek et al. 2003). The difference amounts to about 2σ and could reflect substantial time variability between our Asca observations from 1998 February 11 and the Chandra X-Ray Observatory observations on 2000 September 20. There are also some quantitative differences between the $z_a = 0.524$ DLA system toward AO 0235+164 and Galactic absorption. The dust-to-gas ratio of $k = 0.15 \pm 0.03$ is more similar to that found in the LMC. The dust-to-metals of $k/Z = 0.27 \pm 0.12 (k/Z)_{Galactic}$ is probably not compatible with Galactic in spite of the large possible errors. It is more similar the dust-to-metals of $k/Z = 0.5 (k/Z)_{Galactic}$ estimated from element depletions in much lower metallicity high z DLA systems (Pettini et al. 1997a). The dust at $z_a = 0.524$ may also differ from Galactic dust in the shape of its extinction curve. The dust either has less extinction than Galactic dust at UV wavelengths shortward of $\sim 1700 \text{ \AA}$, or AO 0235+164 has a complex intrinsic spectrum with a steeply rising far-UV part (in νf_ν units) at $\lambda < 1300 \text{ \AA}$ (rest $z_e = 0.94$).

The $z_a = 0.524$ absorption system is not dominated by SMC or LMC like dust because the SMC extinction curve would produce an un-detectable 2175 \AA feature and the LMC extinction curve produces far too much UV extinction relative to the 2175 \AA depth to be a good match to the observed spectrum. Although the extinction due to the dust at $z_a = 0.524$ is closer to Galactic than to that for SMC or LMC, substantial deviations from the family of Galactic extinction curves cannot be ruled out.

The AO 0235+164 $z_a = 0.524$ absorption system provides an excellent illustration of the selection effects due to dust predicted by Pei and Fall (1995). The dust extinction at the observed B band is ~ 1.3 mag, and would result in 91% of such systems being missed in a B magnitude limited quasar survey. Dusty systems such as the AO 0235+164 $z_a = 0.524$ absorber, with $N(HI) = 5 \times 10^{21} \text{ cm}^{-2}$, and $Z = 0.72 Z_\odot$, might contribute a significant fraction to the H I, dust, and metallicity of the Universe as a function of redshift. The dust-to-metals mass ratio of this one system is much less than the Galactic dust-to-metals ratio assumed by Pei and Fall (1995) in calculating the correction for DLA systems obscured by dust. If the dust-to-metals ratio is consistently low in DLA systems, then, perhaps, dusty systems are less important than previously assumed. On the other hand, if one in ten systems has both high metallicity and dust, these systems can dominate the gas and dust phase metal inventory of the Universe. The contribution of dusty systems is still an open question. These observations show that there are dusty systems with properties intermediate

between the low metallicity DLA systems that have been studied previously and our Galaxy.

The authors wish to recognize and acknowledge the very significant cultural role and reverence that the summit of Mauna Kea has always had within the indigenous Hawaiian community. We are most fortunate to have the opportunity to conduct observations from this mountain. Support for this work was provided by: NASA through grant number GO–7294 from the Space Telescope Science Institute, which is operated by AURA, Inc., under NASA contract NAS5–26555; through NASA Chandra program, via Smithsonian Institution grant GO1-2113X, and through Department of Energy contract no. DE-AC03-76SF00515 to the Stanford Linear Accelerator Center.

REFERENCES

- Bechtold, J., Siemiginowska, A., Aldcroft, T., Elvis, M., & Dobrzycki, A. 2001, *ApJ*, 562, 133
- Briggs, F. H. 1987, *QSO Absorption Lines: Probing the Universe*, ed. J. Blades, D. Turnshek, & C. Norman, (Baltimore:STScI), 275
- Briggs, F. H. 1999, *Highly Redshifted Radio Lines*, ASP Conference Series Vol 156, ed. C. I. Carilli, S. J. E. Radford, K. M. Menten, & G. I. Langston, 16
- Burbidge, E. M., Beaver, E. A., Cohen, R. D., Junkkarinen, V. T., and Lyons, R. W. 1996, *AJ*, 112, 2533
- Burbidge, E. M., Caldwell, R. D., Smith, H. E., Liebert, J. and Spinrad, H. 1976, *ApJ*, 205, L117
- Cardelli, J. A., Clayton, G. C., and Mathis, J. S. (CCM) 1989, *ApJ*, 345, 245
- Cohen, R. D., Barlow, T. A., Beaver, E. A., Junkkarinen, V. T., Lyons, R. W., and Smith, H. E. 1994, *ApJ*, 421, 453
- Cohen, R. D., Smith, H. E., Junkkarinen, V. T., and Burbidge, E. M. 1987, *ApJ*, 318, 577
- D’Odorico, S., di Serego Alighieri, S. Pettini, M., Magain, P., Nissen, P. E. et al. 1989, *A&A*, 215, 21
- Diplas, A. and Savage, B. D. 1994, *ApJ*, 427 274
- Draine, B. T., and Malhorta, S. 1993, *ApJ*, 414, 632

- Ellison, S. L., Yan, L., Hook, I. M., Pettini, M., Wall, J. V., and Shaver, P. 2001, *A&A*, 379, 393
- Elvis, M., Lockman, F. J. and Wilkes, B. J. 1989, *AJ*, 97, 777
- Fall, S. M., and Pei, Y. C. 1989, *ApJ*, 337,7
- Fall, S. M., and Pei, Y. C. 1993, *ApJ*, 402, 479
- Fall, S. M., Pei, Y. C., and McMahon, R. G. 1989, *ApJ*, 341, L5
- Fitzpatrick, E. L. 1999, *PASP*, 111, 63
- Fitzpatrick, E. L., and Massa, D. 1986, *ApJ*, 307, 286
- Heckman, T. M., and Lehnert, M. D. 2000, *ApJ*, 537, 690
- Herbig, G. H. 1995, *ARA&A*, 33 , 19
- Hunter, S., et al. 1993, *A&A*, 272, 59
- Krelowski, J., Walker, G. A. H., Grieve, G. R., and Hill, G. M. 1987, *ApJ*, 316, 449
- Lane, W. M., Briggs, F. H., Rao, S. M., and Turnshek, D. A. 1998, *AAS*, 193.0409
- Lanzetta, K. M. and Bowen, D. V. 1992, *ApJ*, 391, 48
- Lu, L., Sargent, W. L. W., Barlow, T. A., Churchill, C. W., and Vogt, S. 1996, *ApJS*, 107, 475
- Madejski, G., Takahashi, T., Tashiro, M., Kubo, H., Hartman, R., Kallman, T., and Sikora, M. 1996, *ApJ*, 459, 156
- Malhotra, S. 1997, *ApJ*, 488, L101
- Marscher, A. P., and Marchenko, S. G. 1999, *BL Lac Phenomenon*, ASP Conference Series Vol 159, ed. L. O. Takalo & A. Sillanpää, 417
- Motta, V., Mediavilla, E., Muñoz, J. A., Falco, E., Kochanek, C. S., Arribas, S., García-Lorenzo, B., Oscoz, A., and Serra-Ricart, M. 2002, *ApJ*, 574, 719
- Nilsson, K., Charles, P. A., Pursimo, T., Takalo, L. O., Sillanpää, A. and Teerikorpi, P. 1996, *A&A*, 314, 754
- Oke, J. B., Cohen, J. G., Carr, M., Cromer, J., Dingizian, A., Harris, F. H., Labrecque, S. Lucinio, R., Schall, W., Epps, H., and Miller, J. 1995, *PASP*, 107, 375

- Pei, Y. C. 1992, ApJ, 395, 130
- Pei, Y. C. and Fall, S. M. 1995, ApJ, 454, 69
- Pei, Y. C., Fall, S. M., and Bechtold, J. 1991, ApJ, 378, 6
- Pei, Y. C., Fall, S. M., and Hauser, M. G. 1999, ApJ, 522, 604
- Pettini, M, King, D. L., Smith, L. J., and Hunstead, R. W. 1997a, ApJ, 478, 536
- Pettini, M, King, D. L., Smith, L. J., and Hunstead, R. W. 1997b, ApJ, 486, 665
- Pettini, M, Smith, L. J., Hunstead, R. W., and King, D. L. 1994, ApJ, 426, 79
- Pettini, M., Ellison, S. L., Steidel, C. C., and Bowen, D. V. 1999, ApJ, 510, 576
- Prantzos, N., and Boissier, S. 2000, MNRAS, 315, 82
- Prochaska, J. X., and Wolfe, A. M. 1999, ApJS, 121, 369
- Prochaska, J. X., and Wolfe, A. M. 2000, ApJ, 533, L5
- Rao, S. M., and Turnshek, D. A. 1998, ApJ, 500, L115
- Rao, S. M., and Turnshek, D. A. 2000, ApJS, 130, 1
- Rieke, G. H., Grasdalen, G. L, Kinman, T. D., Hintzen, P., Wills, B. J., and Wills, D. 1976, Nature, 260, 754
- Roberts, M. S., Brown, R. L., Brundage, W. D., Rots, A. H., Haynes, M. P., and Wolfe A. M. 1976, AJ, 81, 293
- Smith, H. E., Burbidge, E. M., and Junkkarinen, V. T. 1977, ApJ, 218, 611
- Snijders, M. A. J., Boksenberg, A., Penston, M. V., and Sargent, W. L. W. 1982, MNRAS, 201, 801
- Storrie–Lombardi, L. J., Irwin, M. J., and McMahon 1996a, MNRAS, 282, 1330
- Storrie–Lombardi, L. J., Irwin, M. J., and McMahon 1996b, MNRAS, 283, L79
- Turnshek, D. A., Rao, S. M., Ptak, A. F., Griffiths, R. E., and Monier, E. M. 2003, ApJ, 590, 730
- Urry, C. M. 1999, *BL Lac Phenomenon*, ASP Conference Series Vol 159, ed. L. O. Takalo & A. Sillanpää, 3

Vladilo, G., Crivellari, L., Moralo, P., and Beckman, J. E. 1987, *A&A*, 182, L59

Will, L. M., and Aannestad, P. A. 1999, *ApJ*, 526, 242

Wolfe, A. M., Davis, M. M., and Briggs, F. H. 1982, *ApJ*, 259, 495

Womble, D. Junkkarinen, V., Cohen, R., and Burbidge, M. 1990, *AJ*, 100, 1785

Yanny, B., York, D. G., and Gallagher, J. S. 1989 *ApJ*, 338, 735

Fig. 1.— Spectra of AO 0235+164. The upper spectrum is the STIS spectrum obtained 11 February 1998 (UT). All three individual spectra, NUV–MAMA G230L, CCD G430L, and CCD G750L, have been binned 2:1. The lower spectrum shows the Keck LRIS spectrum from 7 November 1997 (UT). The bottom trace shows the 1σ error in the unbinned STIS spectrum

Fig. 2.— The X–ray spectrum of AO 0235+164 from a representative Asca detector as observed on February 11–12, 1998. The spectrum as shown is corrected for the instrumental response. Also shown is a fit using a power law spectrum with absorption due to the Galaxy and the $z_a = 0.524$ absorption system toward AO 0235+164.

Fig. 3.— Confidence regions ($\chi^2_{min} + 2.3, 4.6,$ and 9.2) for the absorption models fitted simultaneously to the ROSAT and 1994 and 1998 Asca data. The ordinates are the columns of the primordial absorber (consisting of H and primordial He) and the chemically processed absorber (no H, and only the processed portion of He, plus all other elements), both parametrized via hydrogen column density of material at solar abundances. The STIS measurement yielding the column of H I of $5 \times 10^{21} \text{ cm}^{-2}$ implies the metallicity of $\sim 0.36/0.5 = 0.72$ solar

Fig. 4.— Spectrum of AO 0235+164 around the $z_a = 0.524$ DLA line. The STIS NUV–MAMA G230L spectrum is shown as a histogram, the one σ errors are shown shifted below the spectrum, and a model obtained from a χ^2 fit to this spectral region with $N(HI) = 5 \times 10^{21} \text{ cm}^{-2}$ is shown as a heavy solid line superposed on the data

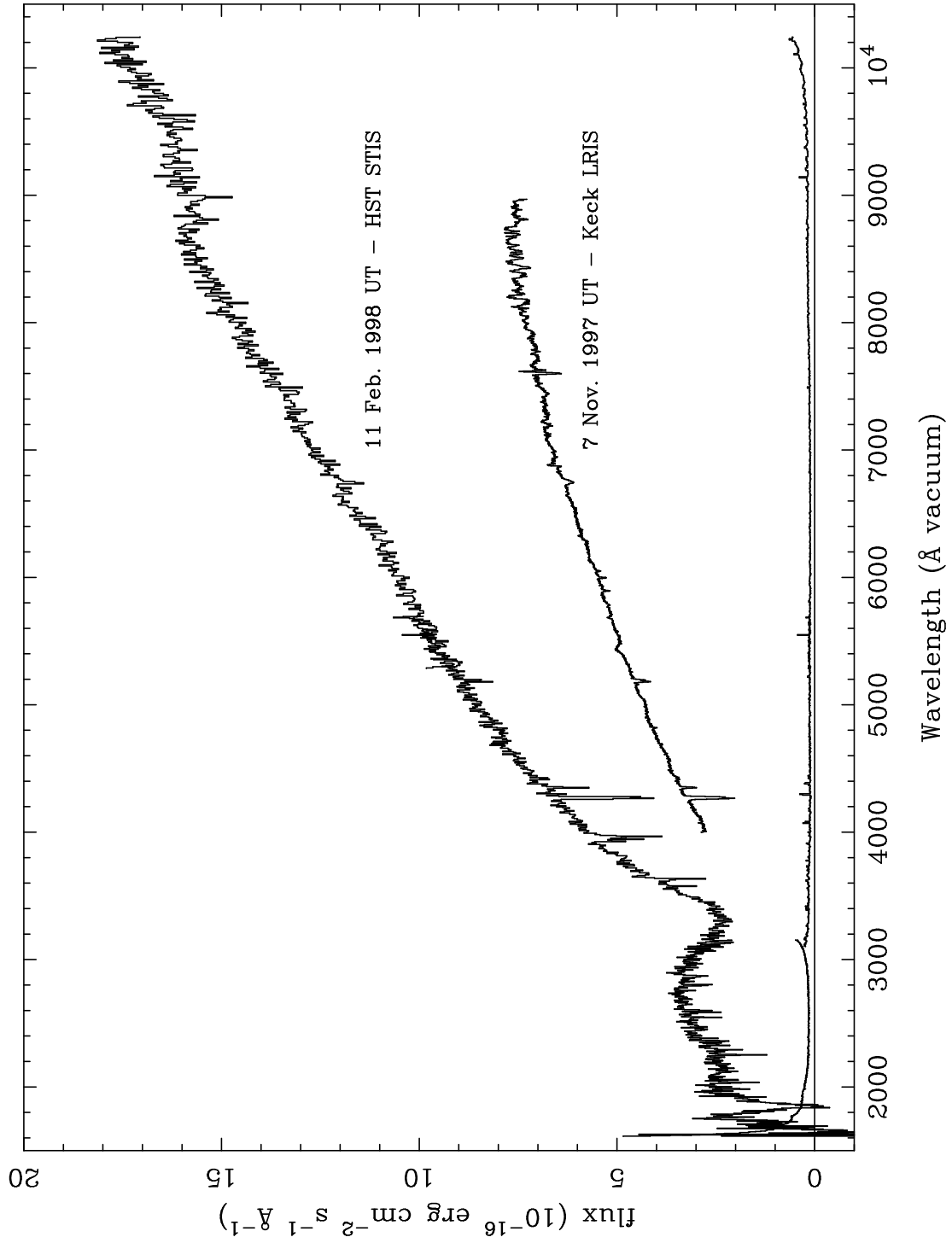
Fig. 5.— HST STIS spectra of AO 0235+164 from Figure 1 and Galactic, LMC, and SMC dust model χ^2 fits. The data are binned 2:1. For clarity, the continua of the fitting functions are shown displaced above the data. Superposed on the data is the Galactic model.

Fig. 6.— The Keck LRIS spectrum of AO 0235+164 showing the spectral region around the $z_a=0.524$ 4428 Å DIB feature. The spectrum is plotted as normalized flux versus wavelength. The zero point for normalized flux is below the lower left corner of the plot in order to display the low contrast DIB feature.

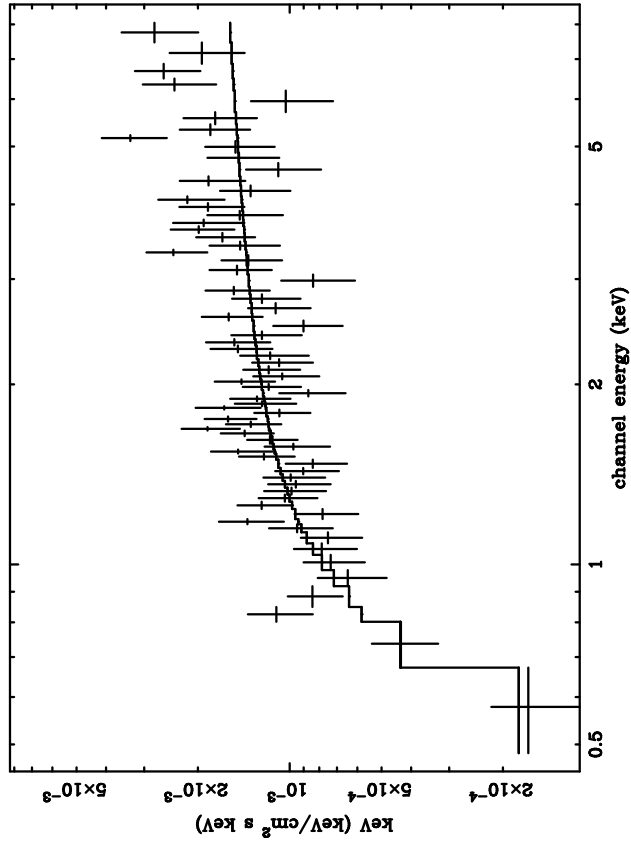
Fig. 7.— The dereddened (upper) and observed (lower) HST STIS spectra of AO 0235+164 shown as flux vs. wavelength. The STIS NUV–MAMA data are binned 3:1 and the STIS CCD data are binned 2:1.

Fig. 8.— The observed (lower) and dereddened (upper – see text for parameters) HST STIS spectra of AO 0235+164 obtained February 11, 1998, shown as $\log_{10}(\nu f_\nu)$ vs $\log_{10}(\nu)$. Also shown is the observed Asca X–ray spectrum from February 11–12, 1998. The data have

been shifted to the rest frame of the $z_e = 0.94$ BL Lac object. The STIS NUV–MAMA data are binned 3:1, the STIS CCD data are binned 2:1, and deep absorption features have been arbitrarily clipped.



(Figure 1)



(Figure 2)

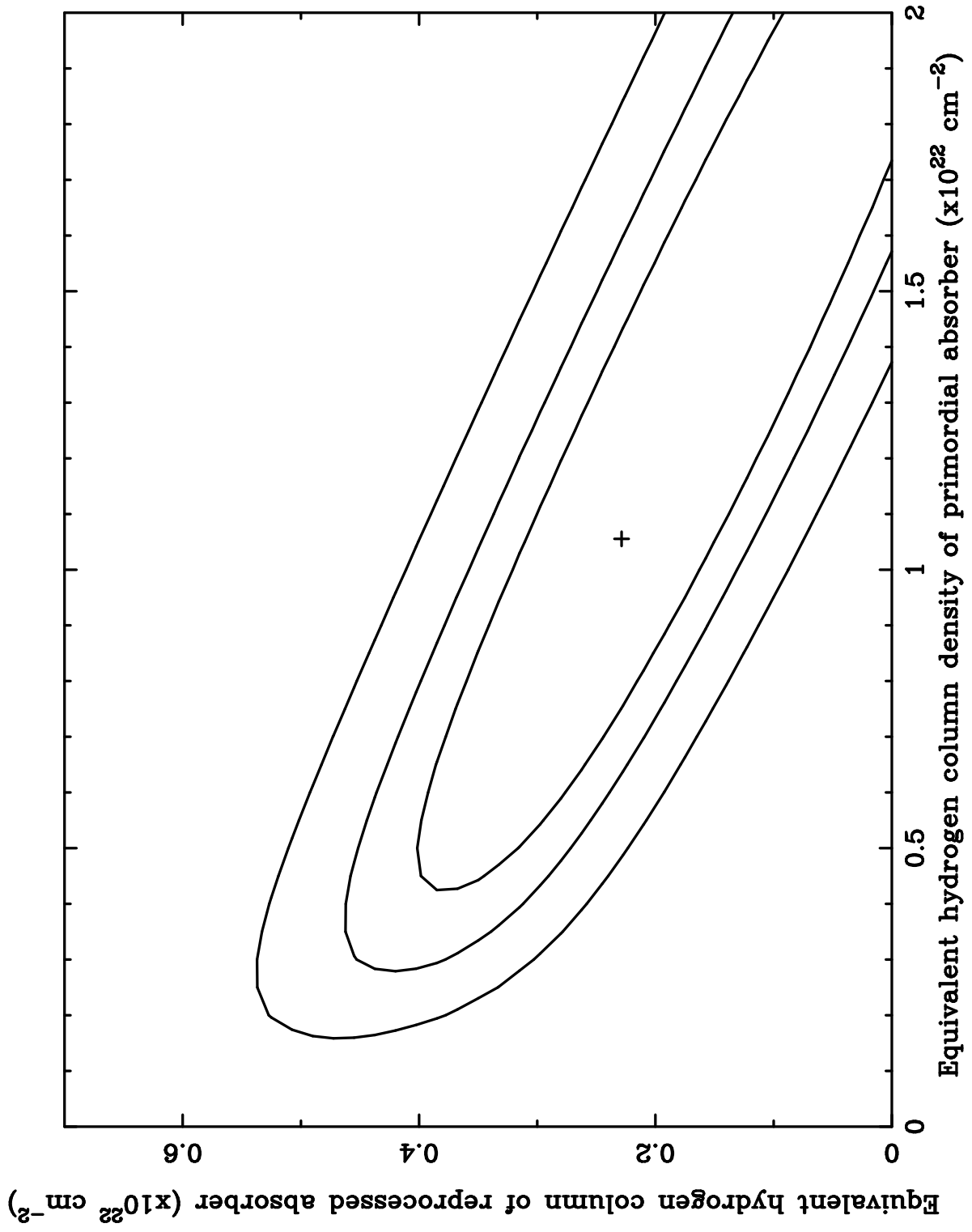


(Figure 3)

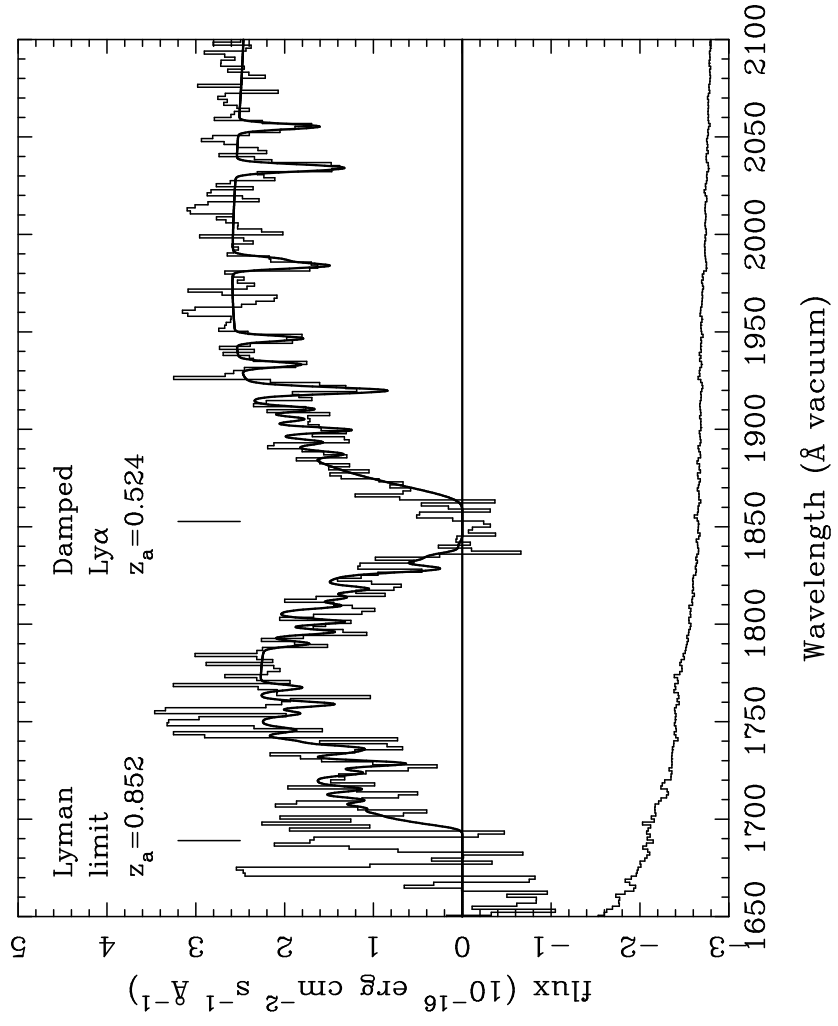


(Figure 4)

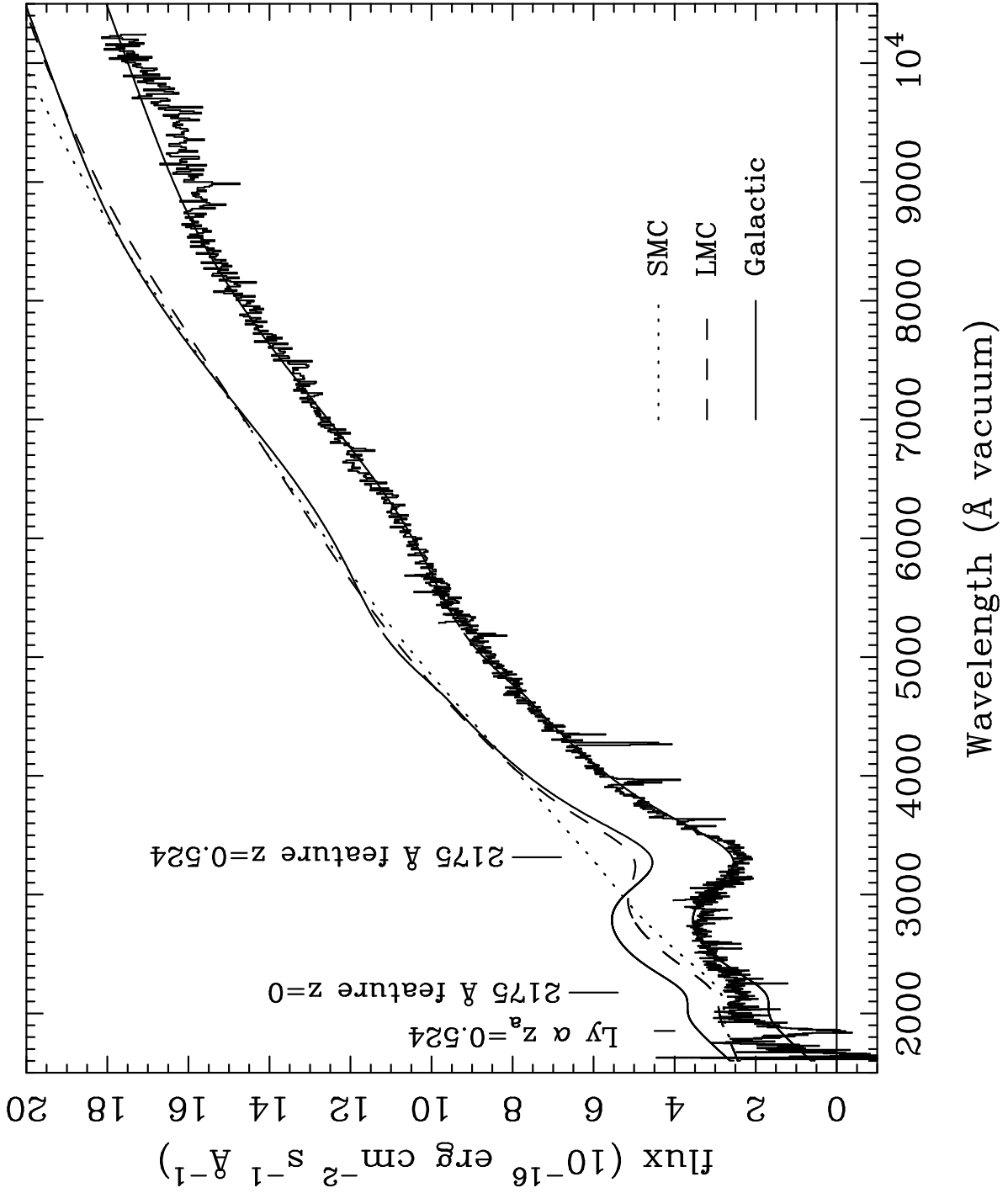


(Figure 5)

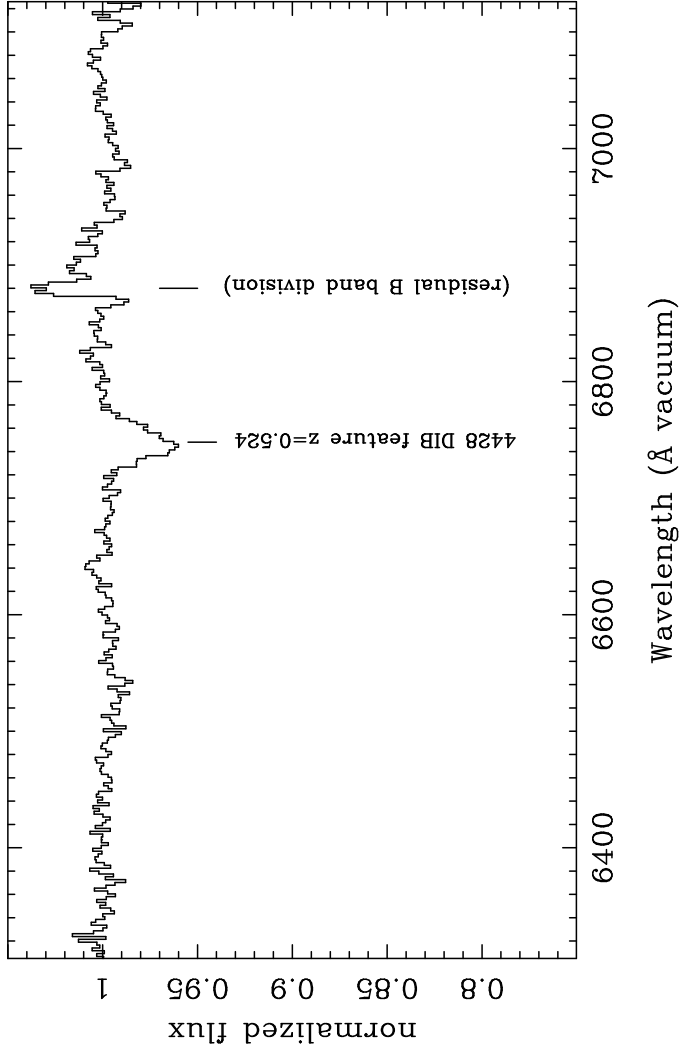


(Figure 6)

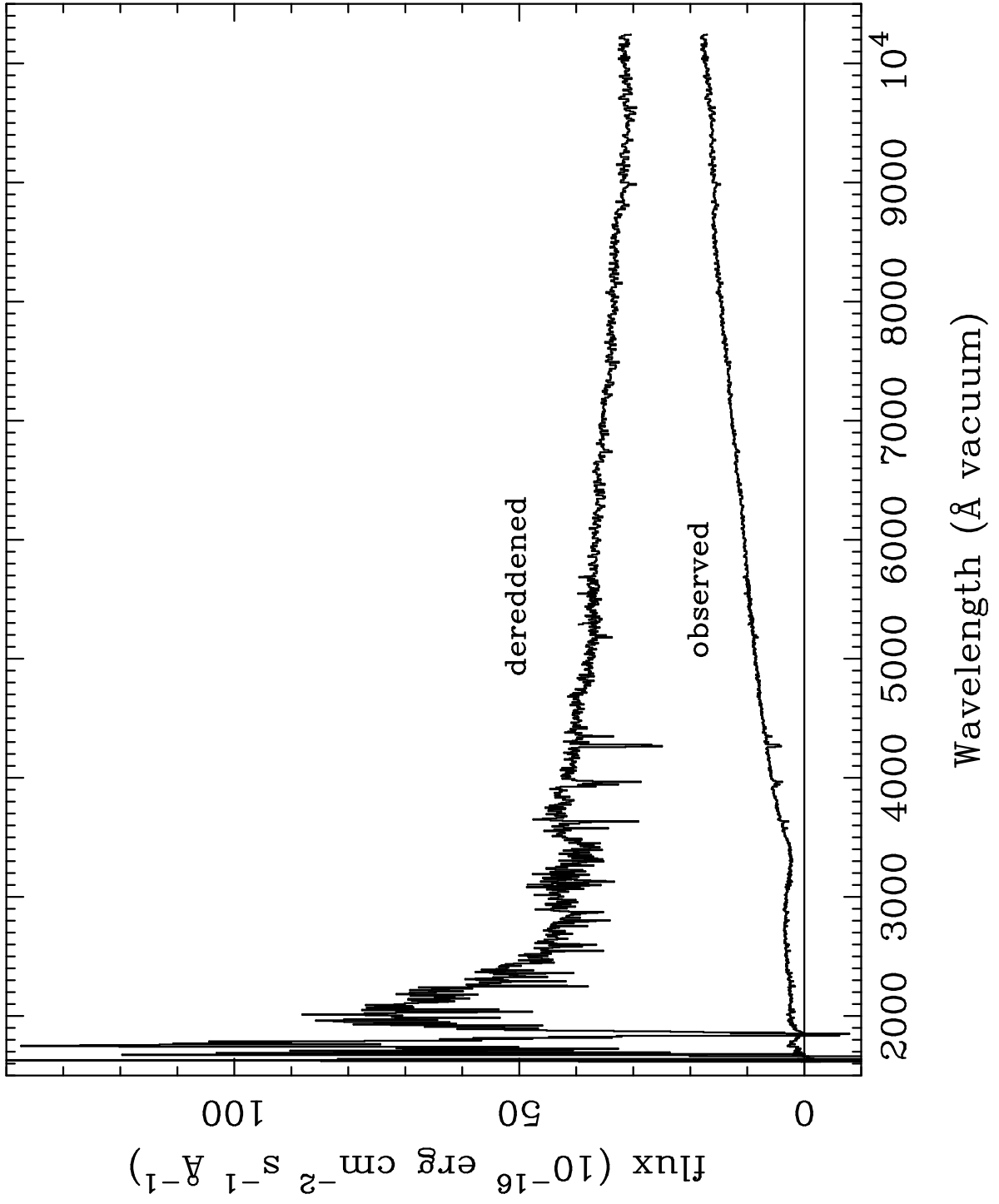


(Figure 7)

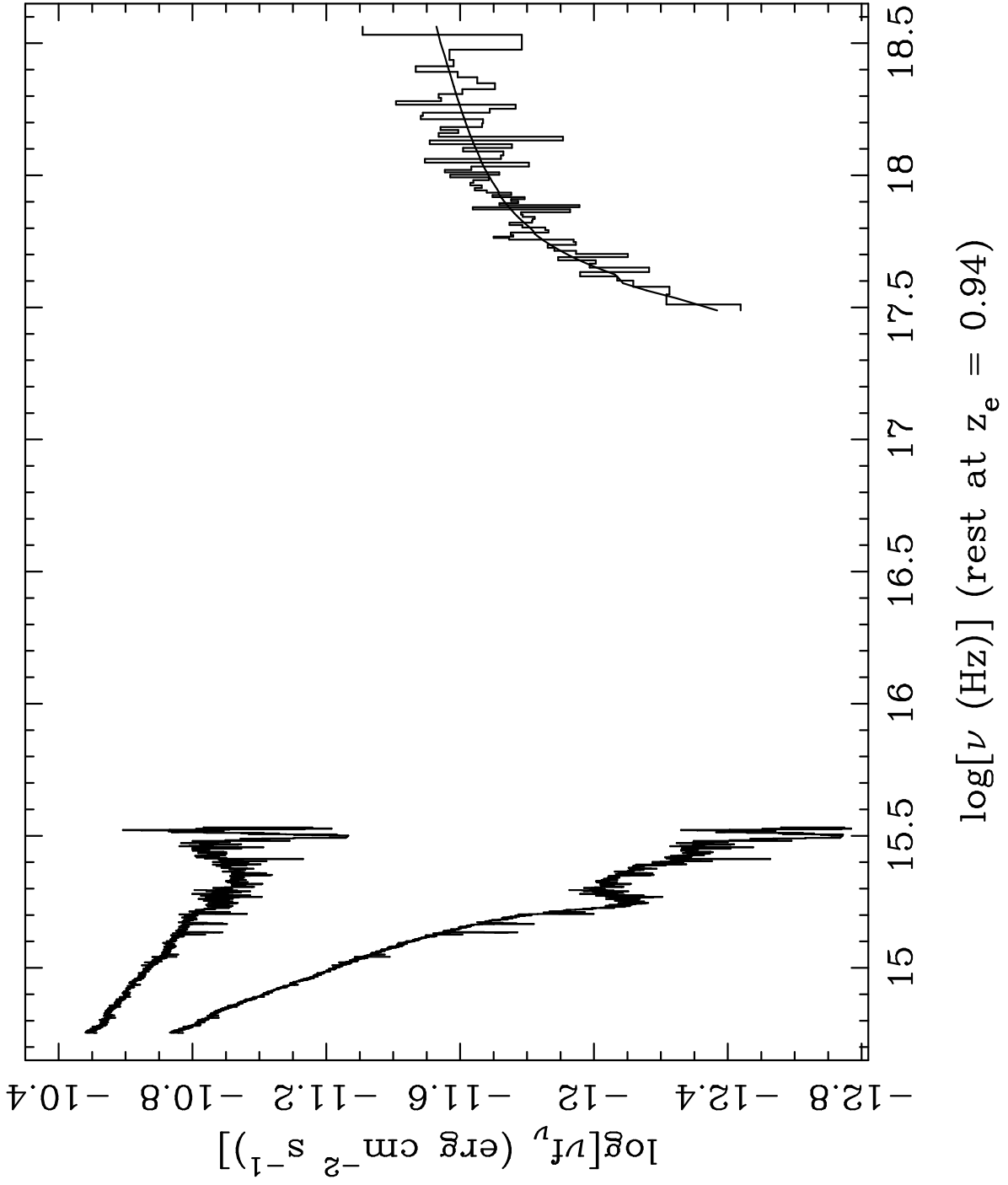


(Figure 8)

TABLE 1
AO 0235+164 Spectral Fits with Dust Extinction

Fit No.	Dust Type	Ref. [†] No.	E(B - V)	$\sigma^{\dagger\dagger}$	R_V	$\sigma^{\dagger\dagger}$	α^{\ddagger}	$\sigma^{\dagger\dagger}$	λ_1^* Å	λ_2^* Å	χ_ν^2
1	Galactic	1	0.227	0.003	2.51	0.03	-1.75	0.01	2500	8700	2.67
2	LMC	2	0.281	0.004	3.16	-	-1.40	0.02	2500	8700	5.31
3	SMC	2	0.161	0.006	2.93	-	-1.63	0.03	2500	8700	14.2
4	LMC	2	0.396	0.005	3.16	-	-0.72	0.03	2800	6000	2.50
5	mod. Gal.**	3	0.211	0.002	3.08	-	-1.76	0.01	1690	8700	3.08
6	Gal.+LMC ^{‡‡}	1+2	0.267	0.003	2.95	0.02	-1.60	0.01	1690	8700	3.72
7	Galactic	1	0.223	0.003	2.43	0.03	-1.75	0.01	2549	8700	2.44
7b							+0.28	0.06	1690	2549	

† Reference for extinction formulae: 1. CCM; 2. Pei (1982); 3 Pei (1982) modified to allow a variable far-UV extinction component. R_V is a fixed value in the models using the Pei (1982) formulae for extinction and a variable in the models using the CCM formulae.

†† Only the formal error – systematic errors probably dominate and are much larger.

‡ Power law spectral index for the continuum modeled as $f_\nu \propto \nu^\alpha$. For model 7 a broken power law was used and the continuum parameters for the blue part are given in line 7b.

* Beginning and end wavelength of the spectral region modeled as a power law and included in the fit.

** A modified Galactic extinction with a reduced far-UV component (see text).

‡‡ A model with both Galactic and LMC type absorbers at $z_a = 0.524$. The best fit found required no LMC type absorption ($E(B - V) \leq 0.005$).